J. Math. Biol. (2018) 76:97–150
https://doi.org/10.1007/s00285-017-1138-1

Mathematical Biology

The kinetics in mathematical models on segmentation clock genes in zebrafish

Kuan-Wei Chen[1] · **Kang-Ling Liao**[2] · **Chih-Wen Shih**[1]

Received: 2 August 2016 / Revised: 26 April 2017 / Published online: 25 May 2017

Abstract Somitogenesis is the process for the development of somites in vertebrate embryos. This process is timely regulated by synchronous oscillatory expression of the segmentation clock genes. Mathematical models expressed by delay equations or ODEs have been proposed to depict the kinetics of these genes in interacting cells. Through mathematical analysis, we investigate the parameter regimes for synchronous oscillations and oscillation-arrested in an ODE model and a model with transcriptional and translational delays, both with Michaelis–Menten type degradations. Comparisons between these regimes for the two models are made. The delay model has larger capacity to accommodate synchronous oscillations. Based on the analysis and numerical computations extended from the analysis, we explore how the periods and amplitudes of the oscillations vary with the degradation rates, synthesis rates, and coupling strength. For typical parameter values, the period and amplitude increase as some synthesis rate or the coupling strength increases in the ODE model. Such variational properties of oscillations depend also on the magnitudes of time delays in delay model. We also illustrate the difference between the dynamics in systems modeled with linear degradation and the ones in systems with Michaelis–Menten type reactions for the degradation. The chief concerns are the connections between the dynamics in

✉ Chih-Wen Shih
cwshih@math.nctu.edu.tw

Kuan-Wei Chen
kwchen0613@gmail.com

Kang-Ling Liao
kangling325@gmail.com

[1] Department of Applied Mathematics, National Chiao Tung University, Hsinchu 300, Taiwan

[2] Department of Biology, The University of North Carolina at Chapel Hill, Chapel Hill, NC, USA

these models and the mechanism for the segmentation clocks, and the pertinence of mathematical modeling on somitogenesis in zebrafish.

Keywords Gene regulation · Segmentation clock gene · Synchronous oscillation · Oscillation-arrested · Delay equation

Mathematics Subject Classification 34K18 · 92B25 · 92C15 · 92C45

1 Introduction

Mathematical modeling for gene regulation can easily go up to multiple or high dimensions, if several genes, their mRNA and protein products are taken into account. Such models can be expressed by coupled nonlinear systems. Aside from the complicated biochemical details, there are time delays involved in the process, including the synthesis of mRNA and proteins, and the modification and transport of molecules. The amount of time lags in these processes may extend to tens of minutes. It is therefore reasonable to incorporate delays into modeling of such processes. Mathematical techniques for analyzing such coupled nonlinear systems with multiple delays become essential in understanding the dynamical properties of those models.

One interesting instance is the modeling of somitogenesis in vertebrate development. Somites are segmental structures arising one by one from the presomitic mesoderm (PSM) and laying along the antero-posterior axis of vertebrate embryos. They later develop, through further differentiation, into vertebrate, rib, and tail. The process during the development of somites is called *somitogenesis*. It involves gene regulation in both space and time. Somite segmentation depends on oscillatory gene expression for cells in the PSM, with neighboring cells oscillating in synchrony. In zebrafish, the involved oscillating genes include *her*1, *her*7, and cells interact through Delta–Notch signaling (Horikawa et al. 2006; Jiang et al. 2000; Mara et al. 2007; Özbudak and Lewis 2008; Riedel-Kruse et al. 2007). Mutations in the Notch cell–cell signaling pathway disrupt synchronization and somite formation and lead to defective somite boundary and irregular segmented body axis (Jiang et al. 2000; Lewis 2003). Therefore, both oscillation and synchronization of clock gene expression are necessary dynamics for normal segmentation. In addition, the oscillation period of clock genes in the tail bud of zebrafish is about 30 min which matches the period of somites made (Hanneman and Westerfield 1989; Holley 2007). This shows that the expressions of the clock genes play an important role in somitogenesis and mathematical model can help understand the processes during somitogenesis.

Autorepression of clock genes by its own protein product has been advocated as the main mechanism for the single cell oscillations in the zebrafish segmentation clock. A simple mathematical model for such regulation involving the mRNA and protein of either *her*1 or *her*7 gene was proposed in Lewis (2003). A key feature of this system is the inclusion of transcriptional and translational time delays. On the other hand, by considering the processes in the cell responsible for time delays, an ODE system was

studied in Uriu et al. (2010). Therein, the transport of Her protein from cytoplasm to nucleus is taken into account, so that the protein concentrations in cytoplasm and nucleus are both state variables. Although many components of the segmentation clock in zebrafish have been identified in the past decade, further detailed regulatory interactions among these components, and the associated biochemical evidences were recently explored. That the core of the clock's regulatory circuit consisting two distinct negative feedback loops, one with Her1 homodimers and the other with Her7:Hes6 heterodimers, was reported in Schröter et al. (2012). More complete models taking into account mRNA molecules of *her*1, *her*7, *hes*6, *delta*C, and their monomer proteins, and dimer proteins have been investigated (Ay et al. 2013, 2014). Further understanding of the transcriptional regulation of each *her*/*hes* gene in the clock was achieved through experiments and computational modeling in Schwendinger-Schreck et al. (2014).

Normal segmentation relies on well-timed oscillation of clock genes and synchronization over neighboring cells. Cell–cell communication via the Delta–Notch signaling synchronizes adjacent cells so that their gene expressions oscillate in phase. However, as pointed out in Uriu et al. (2010), how synchronized oscillation is achieved is not obvious, as Delta protein in a cell stimulates the expression of *her* clock gene in neighboring cells, but the uprising expression of *her* in these cells in turn suppresses their *delta* genes. Mathematical justification of such a mechanism is therefore of interest. On the other hand, it was reported that when the Notch signaling is absent, the clock desynchronization is due to the stochastic dissociation of Her1/7 repressor proteins from the oscillating *her*1/7 autorepressed target genes (Jenkins et al. 2015).

The "clock and wave" mechanism for the formation of somites was first proposed in Cooke and Zeeman (1976). Based on the experimental evidences in Dubrulle et al. (2001), Dubrulle and Pourquié (2002), Pourquié (2004) and Baker et al. (2006) developed a "clock and wavefront" model to investigate pattern formation of somites, which depends on the gradient of FGF8 expression along the antero-posterior axis of vertebrate embryos. That when the boundaries of somites form was later found to be determined by the clock gene (Özbudak and Lewis 2008). To depict the posterior-to-anterior slowing of oscillation rate, Cinquin (2007) proposed a multicellular model for zebrafish somitogenesis that involves heterodimerization of clock proteins Her1 and Her7, with the control protein Hes6; the later interacts with clock proteins and controls the rate of oscillation (Kawamura et al. 2005; Sieger et al. 2006). Campanelli and Gedeon (2010) constructed a delay model extended from Lewis's model to study how the transcription binding sites and decay rates for clock protein monomers and dimers affect the formation of the gene-expression wave. In Uriu et al. (2009), traveling wave solutions on a lattice system consisting of the ODEs with some of the reaction rates formulated in gradient along the lattice was investigated. Contrary to this result, a recent experimental and computational study indicates that Her7 protein degrades uniformly along the PSM (Ay et al. 2014). Instead, it was asserted that an increasing gradient of gene expression time delays from the posterior to the anterior leads to the traveling wave patterns (Ay et al. 2013, 2014). We note that in the mathematical models, linear degradation was adopted in Lewis (2003), Cinquin (2007), Schröter et al. (2012), Ay et al. (2013) and Jenkins et al. (2015), whereas the Michaelis–Menten reaction for degradation was employed in Uriu et al. (2009, 2010). The reason for adopting

Michaelis–Menten reaction is that degradation of proteins generally involves enzymatic reactions. We shall compare these formulations in Sect. 2.

The above-mentioned kinetic models were regarded complicated and difficult to analyze mathematically, as commented in Baker and Schnell (2009). Researchers turned to seek other theoretical framework to encompass both temporal and spatial aspects of somitogenesis. By focussing on the collective behaviors in terms of the phase in a collection of cells clocks, rather than concentrating on the internal machinery of cells, a coupled phase oscillator model has been employed in Morelli et al. (2009) and Herrgen et al. (2010). Such system of phase equations is adapted from the Kuramoto's model which is closely associated with the theory of weakly coupled system for neuronal dynamics (Kuramoto 1984; Ermentrout and Terman 2010). Kuramoto's model was extended to incorporate time delay in Yeung and Strogatz (1999). From this model, under some assumptions, a collective frequency Ω of coupled oscillations was derived to satisfy

$$\Omega = \omega_L - \varepsilon \sin(\Omega\tau), \tag{1}$$

where ω_L is the intrinsic frequency and ε is the coupling strength. Much of the theory and its fit to the experimental data are based on this relationship. While the kinetic models are formulated at the level of single cells, the phase model can be regarded as at the tissue level. However, the connection and correspondence between the kinetic models and phase model have remained elusive, both biologically and mathematically.

Systems modeled with time delays and systems without time delays can certainly exhibit disparate dynamics. In addition, systems employing linear degradation and the ones using Michaelis–Menten degradation can have completely different dynamics. Yet how the reaction rates, delay magnitudes, and coupling strength affect the collective behaviors for each of these systems is a complicated research task. In the context of biological oscillations, dynamical properties for periodic orbits, such as variation of periods and amplitudes with respect to parameters, are key targets. As these mathematical models are differential equations, further mathematical studies shall definitely help understand these models, and provide complements to purely numerical findings. However, developing effective mathematical approach to analyse these models is itself a challenge.

Theoretical analysis on the existence and stability of synchronous periodic solutions for the ODE system proposed in Uriu et al. (2010) is a nontrivial task and has not been reported. This is due to that as the parameters vary, the equilibrium, hence the linearization at the equilibrium, along with its eigenvalues, all change. Nevertheless, it is important to find conditions under which cells can achieve synchronization in a sufficiently short time and to compare models with delay and without delay to clarify which is more suitable to generate stable synchronous oscillations. Oscillation-arrested is another important dynamical mode in the clock gene models. Biologically, we regard this mode as the phase of formed somites in the gene expression. For a nonlinear system in multi-dimensional phase space, it is another task to justify that there does not exist an oscillation. Global convergence to an equilibrium provides such a scenario. However, concluding such a convergence for coupled nonlinear delayed systems requires a new idea, since for example, finding a global Lyapunov function for these systems does not seem possible.

In this paper, we shall perform mathematical analysis to investigate synchronous oscillations and oscillation-arrested for the ODE system proposed by Uriu et al. (2009, 2010) as well as a modified system with delays. We are interested in seeing the dynamics for the coupled cells as well as the parameter values corresponding to synchronous oscillations and global convergence to equilibrium. Hopf bifurcation theory is a natural mathematical tool to analyze the existence and stability of synchronous periodic orbits in the clock gene models. For the ODE system, we demonstrate that there are two parameters, one representing the activation rate (coupling strength), and the other expressing a synthesis rate, and each can serve as a bifurcation parameter in Hopf bifurcation. For the delay system, we use the sum of transcriptional delay and translational delay as the bifurcation parameter in delay Hopf bifurcation theorem, while holding the other parameters suitably fixed. The computation of Hopf bifurcation for delay system is rather involved, especially for the stability of bifurcating periodic orbits, via normal form theory and center manifold theorem. For both systems, under some conditions, we can assert that all solutions remain nonnegative and bounded in forward time. In addition, there exists a unique positive synchronous equilibrium, and a criterion for the global convergence to the synchronous equilibrium can be established by using the sequential-contracting argument developed in Shih and Tseng (2011). Moreover, extended from the mathematical analysis, we shall pursue further numerical findings and illustrate their connections with somitogenesis.

We shall also illustrate the dynamical differences between system modeled with linear degradations and the one with Michaelis–Menten type degradations. Although modeling with Hill-type functions which describe the repression and the Michaelis–Menten type reaction for the degradations result in some complications on the equations, we shall demonstrate that the mathematical analysis for such systems can still be performed. We note that the equations considered in this paper, while serving as basic mathematical models for segmentation clocks in zebrafish, carry typical forms for models describing the kinetics of gene regulation.

The paper is organized as follows. In Sect. 2, we introduce and compare the mathematical models on the segmentation clock gene in zebrafish. In Sect. 3, we show that the solutions remain nonnegative and bounded under some conditions. We then discuss the global convergence to the unique equilibrium. In Sects. 4.1 and 4.2, we discuss synchronous periodic solutions for the ODE system and the delay system, respectively. Several numerical examples which are based on our analytical results are illustrated. In Sect. 5, we compare the dynamics for systems with delays and without delays. We also compare the present results with some previous works. The paper then ends with a conclusion.

2 Cell-to-cell kinetic models

The prevailing models of segmentation clock for zebrafish are based on the mechanism of direct autorepression of the clock gene by its own product and interaction of neighboring cells through positive feedback via Delta–Notch signaling. The basic model contains only one cyclic gene, *her*1 or *her*7. Let x_1, x_2, x_3, x_4 (resp., y_1, y_2, y_3, y_4) represent respectively, the concentrations of *her* mRNA, Her protein, *delta* mRNA,

and Delta protein of the first cell (resp., the second cell). The cell-to-cell kinetic model for the segmentation clock is expressed by

$$\begin{cases} \dot{x}_1(t) = g_H(x_2(t-\tau_1), y_4(t-\tau_1)) - f_1(x_1(t)) \\ \dot{x}_2(t) = a_2 x_1(t-\tau_2) - f_2(x_2(t)) \\ \dot{x}_3(t) = g_D(x_2(t-\tau_3)) - f_3(x_3(t)) \\ \dot{x}_4(t) = a_4 x_3(t-\tau_4) - f_4(x_4(t)) \\ \\ \dot{y}_1(t) = g_H(y_2(t-\tau_1), x_4(t-\tau_1)) - f_1(y_1(t)) \\ \dot{y}_2(t) = a_2 y_1(t-\tau_2) - f_2(y_2(t)) \\ \dot{y}_3(t) = g_D(y_2(t-\tau_3)) - f_3(y_3(t)) \\ \dot{y}_4(t) = a_4 y_3(t-\tau_4) - f_4(y_4(t)). \end{cases} \tag{2}$$

Herein, a_2 (resp., a_4) is the protein synthesis rate per mRNA molecule for *her* (resp., *delta*) gene; $\tau_1,\ \tau_2,\ \tau_3,\ \tau_4$ are the time delays in the processes of *her* gene transcription, *her* gene translation, *delta* gene transcription, *delta* gene translation and delivery to cell membrane, respectively; function g_H relates the transcription initiation rate to the suppression from Her protein and the activation from the Delta protein of neighboring cells; function g_D relates the transcription initiation rate to the suppression from Her protein; $-f_i, i = 1, 2, 3, 4$, represent the degradations. In Lewis (2003) and Özbudak and Lewis (2008), linear degradations are adopted:

$$f_i(x_i) = d_i x_i,\ d_i > 0, \tag{3}$$

and g_H and g_D take the forms

$$g_H(u, v) = k_H \frac{1 + \frac{v}{P_{D_0}}}{1 + \frac{v}{P_{D_0}} + \frac{u^2}{P_0^2}},\ g_D(u) = \frac{k_D}{1 + \frac{u^2}{P_0^2}},\ \text{for } u, v \geq 0, \tag{4}$$

where k_H (resp., k_D) is the maximal synthesis rate of *her* (resp., *delta*) mRNA, and P_0 (resp., P_{D_0}) is the critical number of molecules of Her (resp., Delta) protein per cell for inhibition of transcription (resp., activation of Notch).

With the idea of considering more detailed components of the process and releasing the concern of time delays, an ODE model was proposed and studied in Uriu et al. (2009, 2010). Therein, the process of Her protein transport from cytoplasm to nucleus is taken into account so that Her protein is decomposed into two components: Her protein in cytoplasm and Her protein in nucleus. Let x_1, x_2, x_3, x_4, x_5 (resp., y_1, y_2, y_3, y_4, y_5) be the concentrations of *her* mRNA, Her protein in cytoplasm, Her protein in nucleus, *delta* mRNA, and Delta protein of the first cell (resp., the second cell), respectively. The kinetics of gene regulation was modeled by

$$\begin{cases} \dot{x}_1(t) = g_H(x_3(t), y_5(t)) - f_1(x_1(t)) \\ \dot{x}_2(t) = \nu_3 x_1(t) - f_2(x_2(t)) \\ \dot{x}_3(t) = \nu_5 x_2(t) - f_3(x_3(t)) \\ \dot{x}_4(t) = g_D(x_3(t)) - f_4(x_4(t)) \\ \dot{x}_5(t) = \nu_9 x_4(t) - f_5(x_5(t)) \\ \\ \dot{y}_1(t) = g_H(y_3(t), x_5(t)) - f_1(y_1(t)) \\ \dot{y}_2(t) = \nu_3 y_1(t) - f_2(y_2(t)) \\ \dot{y}_3(t) = \nu_5 y_2(t) - f_3(y_3(t)) \\ \dot{y}_4(t) = g_D(y_3(t)) - f_4(y_4(t)) \\ \dot{y}_5(t) = \nu_9 y_4(t) - f_5(y_5(t)), \end{cases} \tag{5}$$

where ν_3 and ν_9 are the synthesis rates of Her protein in cytoplasm and Delta protein, respectively, and ν_5 is the transportation rate of Her protein from cytoplasm to nucleus. In addition, g_H and g_D are defined by

$$g_H(u, v) = \frac{k_1^n}{k_1^n + u^n} \cdot (\nu_1 + \nu_c v), \ g_D(u) = \nu_7 \frac{k_7^h}{k_7^h + u^h}, \text{ for } u, v \geq 0, \tag{6}$$

where h and n are the Hill coefficients related to the dimerization process of Her proteins and the number of Her protein binding sites on DNA (Zeiser et al. 2007); ν_1 is the Basal transcription rate of *her* mRNA, ν_c is the activation rate of *her* mRNA transcription by Delta–Notch signal, ν_7 is the synthesis rate of *delta* mRNA, and k_1 and k_7 are the threshold constants for the suppression of *her* mRNA and *delta* mRNA transcriptions by Her protein in nucleus, respectively. As degradation of proteins generally involves enzymatic reactions, the Michaelis–Menten type reactions were adopted therein:

$$\begin{aligned} f_1(u) &= \frac{\nu_2 u}{k_2 + u}, \ f_2(u) = \frac{\nu_4 u}{k_4 + u} + \nu_5 u, \\ f_3(u) &= \frac{\nu_6 u}{k_6 + u}, \ f_4(u) = \frac{\nu_8 u}{k_8 + u}, \ f_5(u) = \frac{\nu_{10} u}{k_{10} + u}, \ \text{ for } u \geq 0, \end{aligned} \tag{7}$$

where ν_2, ν_4, ν_6, ν_8, ν_{10} (resp., $k_2, k_4, k_6, k_8, k_{10}$) are the maximum degradation rates (resp., Michaelis constants for the degradation) of *her* mRNA, Her protein in cytoplasm, Her protein in nucleus, *delta* mRNA, and Delta protein, respectively. Note that f_2 contains the degradation term $\nu_4 u/(k_4 + u)$ and the translocation term $\nu_5 u$. More detailed explanations for employing Michaelis–Menten type degradation in the modeling can be found in Uriu et al. (2009).

A simplified model which combines the two equations for *delta* mRNA and Delta protein into merely one equation for Delta protein was also investigated in Uriu et al. (2010). This reduction led to a system of eight ODEs:

$$\begin{cases} \dot{x}_1(t) = g_H(x_3(t), y_4(t)) - f_1(x_1(t)) \\ \dot{x}_2(t) = \nu_3 x_1(t) - f_2(x_2(t)) \\ \dot{x}_3(t) = \nu_5 x_2(t) - f_3(x_3(t)) \\ \dot{x}_4(t) = g_D(x_3(t)) - f_4(x_4(t)) \\ \\ \dot{y}_1(t) = g_H(y_3(t), x_4(t)) - f_1(y_1(t)) \\ \dot{y}_2(t) = \nu_3 y_1(t) - f_2(y_2(t)) \\ \dot{y}_3(t) = \nu_5 y_2(t) - f_3(y_3(t)) \\ \dot{y}_4(t) = g_D(y_3(t)) - f_4(y_4(t)), \end{cases} \tag{8}$$

where g_D relates both the transcription and translation initiation rates to Delta protein concentration, and is still defined by (6); f_4 is now the degradation for Delta protein, and is defined in (7). In addition, in this model, ν_7 is the synthesis rate of Delta protein, k_7 is the threshold constant for the suppression of Delta protein synthesis by Her protein, ν_8 is the maximum degradation rate of Delta protein, and k_8 is the Michaelis constant for Delta protein degradation in nucleus. It was reported therein that both of these two ODE models (5) and (8) exhibit the main feature of *her* gene regulation and the parameter regimes of stable synchronous periodic solution are much alike.

Models containing more components of the segmentation clock have been studied in Cinquin (2007), Schröter et al. (2012), Ay et al. (2013, 2014) and Jenkins et al. (2015). For example, there are 44 parameters and 14 equations in each cell in the model investigated in Ay et al. (2013, 2014), taking into account the mRNA molecules of *her*1, *her*7, *hes*6, *delta*C, and their monomer proteins and dimer proteins. The degradations in these models were all formulated in the form of linear functions (3).

A chief goal in modeling the segmentation clock is to be able to generate oscillatory traveling wave patterns along the PSM. The wave starts from synchronous oscillation at posterior of PSM, and then the oscillation slows down near the anterior of PSM, and is finally arrested at the anterior of PSM. This can be achieved by considering a lattice of cells, with a pertinent gradient of reaction rates or time delays along PSM. Recently, it has been found that increasing effective time delays along the PSM is responsible for the generation of traveling segmentation clock waves (Ay et al. 2013, 2014). An experimental evidence therein runs against some of the results in Uriu et al. (2009) where the gradient of a degradation rate was formulated to generate traveling waves. On the one hand, periods and amplitudes of oscillations depend also on other parameters. On the other hand, the dynamics in systems with linear degradations can be very different from the ones in systems with Michaelis–Menten type degradations. We shall illustrate this by an example in Sect. 4. Mathematical analysis with numerical simulation extended from the analysis is our approach for exploring how periods of oscillations are influenced by parameters.

A formal linearization of system (8) around an equilibrium was performed and the characteristic equation was derived in Uriu et al. (2010). However, the bifurcation analysis was not completed therein, as there are too many variables and parameters in the system. Therefore, basically, the results therein were obtained by numerical simulations on the ODE systems (5) and (8). However, there are insufficiencies for using purely numerical computations to find periodic solutions for systems with more

than ten parameters in phase space of high dimension, as mentioned in Uriu et al. (2010). In this paper, we shall illustrate that such analysis can be performed, even though the equilibrium of nonlinear system (8) can not be computed exactly. The analysis will then lead to a theoretical support of the existence and stability of the synchronous periodic solutions. We shall also demonstrate that the parameter range for synchronous oscillations adopted in Uriu et al. (2010) can be interpreted within the Hopf bifurcation framework.

Examining and comparing whether the model with time delay or without time delay is more suitable for generating stable synchronous oscillation for the segmentation clock are very interesting in mathematical modeling on somitogenesis. We echo this interest and investigate the following system obtained by adding time delays into (8):

$$\begin{cases} \dot{x}_1(t) = g_H(x_3(t-\tau_1), y_4(t-\tau_1)) - f_1(x_1(t)) \\ \dot{x}_2(t) = \nu_3 x_1(t-\tau_2) - f_2(x_2(t)) \\ \dot{x}_3(t) = \nu_5 x_2(t) - f_3(x_3(t)) \\ \dot{x}_4(t) = g_D(x_3(t-\tau_4)) - f_4(x_4(t)) \\ \\ \dot{y}_1(t) = g_H(y_3(t-\tau_1), x_4(t-\tau_1)) - f_1(y_1(t)) \\ \dot{y}_2(t) = \nu_3 y_1(t-\tau_2) - f_2(y_2(t)) \\ \dot{y}_3(t) = \nu_5 y_2(t) - f_3(y_3(t)) \\ \dot{y}_4(t) = g_D(y_3(t-\tau_4)) - f_4(y_4(t)). \end{cases} \tag{9}$$

Herein, τ_1, τ_2, τ_4 represent respectively the time delays in the processes of *her* gene transcription, *her* gene translation, and *delta* gene transcription, translation, and delivery to cell membrane. We neglect the time delay in the translocation process in the third equation, as the time scale of the translocation is much smaller than the transcription and translation (Görlich and Kutay 1999; Makarov 2009; Simon et al. 1992).

Let us compare the above-mentioned models:

(i) The transcription initiation rate for *her*, $g_H(u, v)$, which plays the role of coupling function, is bounded in (4), but unbounded in (6).
(ii) The degradation terms in (3) are linear and unbounded, whereas the ones in (7) are bounded but in more complicated nonlinear form.
(iii) Transcription and translation time delays are taken into account in system (2) and system (9).
(iv) The translocation process is included in systems (5), (8), and (9), where Her protein is decomposed into Her protein in cytoplasm and Her protein in nucleus.
(v) The Hill coefficients are formulated in g_H and g_D in (6). Their values are determined from dimerization process and DNA binding sites. Functions g_H and g_D in (4) only represent the inhibitory protein as a dimer.

An analytical study for delay system (2) with degradation (3) and transcription function (4) was reported in Liao et al. (2012). Designed from this delay model, a nonautonomous lattice system which can generate normal traveling wave pattern was presented in Liao and Shih (2012). In this work, we shall analyze ODE system (8) and delay system (9), with transcription functions (6) and Michaelis–Menten type

degradation (7). Our analysis can be extended to treat system (9) modified by adding translocation time delay and system (5) modified with time delays incorporated.

3 Basic properties and global dynamics

In this section, we discuss the basic properties for systems (8) and (9), with transcription (6) and degradation (7), to ensure that they are proper in modeling gene regulation. In particular, we shall assure that the mRNA concentrations and their protein products remain nonnegative along time. We also want to confirm that their solutions remain bounded throughout the evolutions. In addition, we shall discuss the existence of synchronous equilibrium and derive globally convergence to this equilibrium. Such convergence excludes oscillation and provides a regime for oscillation-arrested. The properties discussed for system (9) in this section are also valid for system (8), as system (9) reduces to (8) when the delays are zero: $\tau_1 = \tau_2 = \tau_4 = 0$.

The coupled system (9) has three time delays τ_1, τ_2, and τ_4. Fundamental theory for delay equations is established on the infinite-dimensional phase space $\mathscr{C}([-\tau_M, 0], \mathbb{R}^8_+)$, the space of continuous functions from $[-\tau_M, 0]$ to $\mathbb{R}^8_+$, where

$$\tau_M := \max\{\tau_1, \tau_2, \tau_4\},$$
$$\mathbb{R}^8_+ := \{(x_1, \ldots, x_4, y_1, \ldots, y_4) | x_i \geq 0, y_i \geq 0, i = 1, \ldots, 4\}.$$

Let $\Psi(t, \phi)$ be the flow map of (9) which depicts the evolution of the system at time t from initial condition $\phi = (\phi_1, \ldots, \phi_8) \in \mathscr{C}([-\tau_M, 0], \mathbb{R}^8_+)$ at initial time $t_0 = 0$. Denote by $\mathbb{X}(t; \phi)$ the solution induced from (9), i.e., $\mathbb{X}(t + \theta; \phi) = \Psi(t, \phi)(\theta)$, for $\theta \in [-\tau_M, 0]$, and $t > 0$. We also denote $\mathbb{X}(t) = (\mathbf{x}(t), \mathbf{y}(t)) = \mathbb{X}(t; \phi) = (\mathbf{x}(t; \phi), \mathbf{y}(t; \phi))$, where $\mathbf{x} = (x_1, x_2, x_3, x_4)$, $\mathbf{y} = (y_1, y_2, y_3, y_4)$, if ϕ is not specified. When $\tau_1 = \tau_2 = \tau_4 = 0$, system (9) reduces to ODEs (8), with phase space $\mathbb{R}^8_+$.

The following proposition ensures that the mRNA concentrations and their protein products remain non-negative along evolution.

Proposition 1 *$\mathscr{C}([-\tau_M, 0], \mathbb{R}^8_+)$ is positively invariant under the flow generated by system (9), provided that the Hill coefficients h and n are even integers.*

Proof Assume that $h = 2\tilde{h}$ and $n = 2\tilde{n}$ for $\tilde{h}, \tilde{n} \in \mathbb{N}$. We shall show that $x_i(t) \geq 0, y_i(t) \geq 0, i = 1, \ldots, 4$, for solution $\mathbb{X}(t) = \mathbb{X}(t; \phi)$ evolved from an arbitrary $\phi \in \mathscr{C}([-\tau_M, 0], \mathbb{R}^8_+)$. Let $I = I(\phi)$ be the maximal interval of existence for $\mathbb{X}(t; \phi)$.

First,

$$\dot{y}_4(t) = \nu_7 \frac{k_7^{2\tilde{h}}}{k_7^{2\tilde{h}} + y_3^{2\tilde{h}}(t - \tau_4)} - \frac{\nu_8 y_4(t)}{k_8 + y_4(t)} > -\frac{\nu_8 y_4(t)}{k_8 + y_4(t)},$$

for all $t \in I$, since $g_D(u) > 0$, for any $u \in \mathbb{R}$. The solution for $\dot{u}(t) = -\frac{\nu_8 u(t)}{k_8 + u(t)}$ remains nonnegative for all $t \geq 0$, if $u(0) \geq 0$. Hence, $y_4(t) \geq 0$ if $y_4(0) \geq 0$, for all $t \in I$, by comparison arguments. Similarly, we obtain $x_4(t) \geq 0$, for all $t \in I$, from

symmetry of system (9). With $x_4(t), y_4(t) \geq 0$ for all $t \in I$, we use similar argument to derive $x_1(t), y_1(t) \geq 0$, for all $t \in I$. Hence, for $x_2(t)$, we have $\dot{x}_2(t) \geq -\frac{\nu_4 x_2(t)}{k_4 + x_2(t)}$. Thus, $x_2(t) \geq 0$ for all $t \in I$, if $x_2(0) \geq 0$. Similarly and successively, we conclude $y_2(t), x_3(t), y_3(t) \geq 0$, for all $t \in I$, if $x_2(0), x_3(0), y_3(0) \geq 0$. □

Next we derive a condition for the existence of an attracting set for system (9) in the following proposition. Notice that the degradation functions f_i in (7) are bounded, whereas the transcription function g_H in (6) is unbounded. The following quantities will be used to estimate the globally attracting set:

$$\begin{aligned}
\hat{q}_1 &:= \frac{(\nu_1 + \nu_c \hat{q}_4) k_2}{\nu_2 - (\nu_1 + \nu_c \hat{q}_4)}, \\
\hat{q}_2 &:= \frac{\nu_3 \hat{q}_1 - \nu_4 - k_4 \nu_5 + \sqrt{4 k_4 \nu_3 \nu_5 \hat{q}_1 + (\nu_4 + k_4 \nu_5 - \nu_3 \hat{q}_1)^2}}{2\nu_5}, \\
\hat{q}_3 &:= \frac{k_6 \nu_5 \hat{q}_2}{\nu_6 - \nu_5 \hat{q}_2}, \\
\hat{q}_4 &:= \frac{k_8 \nu_7}{\nu_8 - \nu_7}, \qquad (10) \\
\check{q}_1 &:= \frac{k_1^n k_2 \nu_1}{\nu_2 \hat{q}_3^n + k_1^n (\nu_2 - \nu_1)}, \\
\check{q}_2 &:= \frac{\nu_3 \check{q}_1 - \nu_4 - k_4 \nu_5 + \sqrt{4 k_4 \nu_3 \nu_5 \check{q}_1 + (\nu_4 + k_4 \nu_5 - \nu_3 \check{q}_1)^2}}{2\nu_5}, \\
\check{q}_3 &:= \frac{k_6 \nu_5 \check{q}_2}{\nu_6 - \nu_5 \check{q}_2}, \\
\check{q}_4 &:= \frac{k_7^h k_8 \nu_7}{\nu_8 \hat{q}_3^h + k_7^h (\nu_8 - \nu_7)}. \qquad (11)
\end{aligned}$$

Proposition 2 *Assume that h and n are even integers. If*

$$\nu_8 > \nu_7, \ \ \nu_2 > \nu_1 + \nu_c \hat{q}_4, \ \ \text{and } \nu_6 > \nu_5 \hat{q}_2, \qquad (12)$$

then there exists a closed and bounded set $\mathcal{Q} := \Pi_{i=1}^4 Q_i \times \Pi_{i=1}^4 Q_i \subset \mathbb{R}_+^8$, *such that* $\mathbb{X}(t; \phi)$ *converges to* $\mathcal{Q}$ *for any* $\phi \in \mathscr{C}([-\tau_M, 0], \mathbb{R}_+^8)$, *where* $Q_i := [\check{q}_i, \hat{q}_i]$, *with* $\hat{q}_i$, $\check{q}_i$, $i = 1, \ldots, 4$, *defined in* (10) *and* (11).

Proof The idea is to perform component estimation sequentially. With $x_i(t), y_i(t) \geq 0$, $i = 1, \ldots, 4$, from Proposition 1, we have

$$\begin{aligned}
\frac{-\nu_8 y_4(t)}{k_8 + y_4(t)} < \dot{y}_4(t) &= \nu_7 \frac{k_7^h}{k_7^h + y_3^h(t - \tau_4)} - \frac{\nu_8 y_4(t)}{k_8 + y_4(t)} \\
&\leq \nu_7 - \frac{\nu_8 y_4(t)}{k_8 + y_4(t)}, \qquad (13)
\end{aligned}$$

for all $t \in I$. It follows that $y_4(t)$ exists on $[0, \infty)$ and converges to $[0,\ k_8\nu_7/(\nu_8 - \nu_7)] =: [0, \hat{q}_4] =: \tilde{Q}_4$, as $t \to \infty$, due to $\nu_8 > \nu_7$. Subsequently, for an $\epsilon > 0$, there exists a $t_1^\epsilon > 0$ such that

$$\frac{-\nu_2 x_1(t)}{k_2 + x_1(t)} < \dot{x}_1(t) < \nu_1 + \nu_c(\hat{q}_4 + \epsilon) - \frac{\nu_2 x_1(t)}{k_2 + x_1(t)},\ \text{for } t \geq t_1^\epsilon.$$

Therefore, $x_1(t)$ exists on $[0, \infty)$ and converges to $[0,\ k_2(\nu_1 + \nu_c(\hat{q}_4 + \epsilon))/(\nu_2 - (\nu_1 + \nu_c(\hat{q}_4 + \epsilon)))]$ for all $\epsilon > 0$, and hence converges to $[0,\ k_2(\nu_1 + \nu_c\hat{q}_4)/(\nu_2 - (\nu_1 + \nu_c\hat{q}_4))] =: [0, \hat{q}_1] =: \tilde{Q}_1$, as $t \to \infty$, due to $\nu_2 > \nu_1 + \nu_c\hat{q}_4$. Similarly, we can confirm that $x_2(t)$ and $x_3(t)$ exist on $[0, \infty)$ and converge to

$$\left(0, \frac{\nu_3\hat{q}_1 - \nu_4 - k_4\nu_5 + \sqrt{4k_4\nu_3\nu_5\hat{q}_1 + (\nu_4 + k_4\nu_5 - \nu_3\hat{q}_1)^2}}{2\nu_5}\right) =: (0, \hat{q}_2) =: \tilde{Q}_2$$

$$\left(0, \frac{k_6\nu_5\hat{q}_2}{\nu_6 - \nu_5\hat{q}_2}\right) =: (0, \hat{q}_3) =: \tilde{Q}_3,$$

respectively, due to $\nu_6 > \nu_5\hat{q}_2$. In addition, by the symmetry of system (9), $x_4(t)$, $y_1(t)$, $y_2(t)$, $y_4(t)$ also exist on $[0, \infty)$ and converge to sets $\tilde{Q}_4$, $\tilde{Q}_1$, $\tilde{Q}_2$, $\tilde{Q}_3$, respectively.

Next, according to the convergence of $x_3(t)$ to $\tilde{Q}_3$ and $y_4(t)$ to $\tilde{Q}_4$, for any given $\epsilon > 0$, there exists a $t_2^\epsilon > t_1^\epsilon$ such that

$$g_H(x_3(t - \tau_1), y_4(t - \tau_1)) > \frac{k_1^n\nu_1}{k_1^n + \hat{q}_3^n} - \epsilon,\ \text{for all } t > t_2^\epsilon - \tau_M > 0.$$

Therefore,

$$\frac{k_1^n\nu_1}{k_1^n + \hat{q}_3^n} - \epsilon - \frac{\nu_2 x_1(t)}{k_2 + x_1(t)} < \dot{x}_1(t) < \nu_1 + \nu_c(\hat{q}_4 + \epsilon) - \frac{\nu_2 x_1(t)}{k_2 + x_1(t)},\ \text{for all } t \geq t_2^\epsilon.$$

Hence, $x_1(t)$ converges to $[\check{q}_1, \hat{q}_1] =: Q_1$, as $t \to \infty$, with $\check{q}_1 := k_1^n k_2\nu_1/(\hat{q}_3^n\nu_2 + k_1^n(\nu_2 - \nu_1))$. By similar arguments, we can see that $x_2(t)$, $x_3(t)$, $x_4(t)$ converge to $Q_2 := [\check{q}_2, \hat{q}_2]$, $Q_3 := [\check{q}_3, \hat{q}_3]$, $Q_4 := [\check{q}_4, \hat{q}_4]$, respectively, with

$$\check{q}_2 := \frac{\nu_3\check{q}_1 - \nu_4 - k_4\nu_5 + \sqrt{4k_4\nu_3\nu_5\check{q}_1 + (\nu_4 + k_4\nu_5 - \nu_3\check{q}_1)^2}}{2\nu_5},$$

$$\check{q}_3 := \frac{k_6\nu_5\check{q}_2}{\nu_6 - \nu_5\check{q}_2},$$

$$\check{q}_4 := \frac{k_7^h k_8\nu_7}{\nu_8\hat{q}_3^h + k_7^h(\nu_8 - \nu_7)}.$$

In addition, $y_i(t)$ converges to Q_i, $i = 1, \ldots, 4$, via the symmetry of system (9). □

Remark 1 (i) According to Propositions 1 and 2, if Hill coefficients h and n are even, then under the conditions of Proposition 2, every solution of (9) exists on $[0, \infty)$, and is bounded with nonnegative components. There are examples where solutions blow up when the conditions of Proposition 2 are violated.

(ii) We have performed only two iteration steps in the proof of Proposition 2 to obtain an estimate for the attracting region. By continuing this process, the asymptotic dynamics can be captured in even smaller regions. Therefore, we can assert that every solution $\mathbb{X}(t)$ lies in $\mathscr{Q}$ after large time.

We say that an equilibrium $(x_1^*, \ldots, x_4^*, y_1^*, \ldots, y_4^*)$ of (9) is *synchronous* if $x_i^* = y_i^*$, $i = 1, \ldots, 4$. Note that delay system (9) and ODE system (8) share identical equilibrium points. Next, we discuss synchronous equilibrium point for system (9).

Proposition 3 *Assume $\nu_8 > \nu_7$. For any fixed integers $h \geq 1$ and $n \geq 1$, there exists a unique positive synchronous equilibrium point*

$$\bar{\mathbb{X}} = (\bar{\mathbf{x}}, \bar{\mathbf{x}}) = (\bar{x}_1, \bar{x}_2, \bar{x}_3, \bar{x}_4, \bar{x}_1, \bar{x}_2, \bar{x}_3, \bar{x}_4)$$

for system (9), where

$$\begin{aligned}
\bar{x}_1 &= \frac{\nu_6 \bar{x}_3 (k_6(\nu_4 + k_4\nu_5) + (\nu_4 + k_4\nu_5 + \nu_6)\bar{x}_3)}{\nu_3(k_6 + \bar{x}_3)(\nu_6\bar{x}_3 + k_4\nu_5(k_6 + \bar{x}_3))}, \\
\bar{x}_2 &= \frac{\nu_6 \bar{x}_3}{\nu_5(k_6 + \bar{x}_3)}, \\
\bar{x}_4 &= \frac{k_7^h k_8 \nu_7}{k_7^h(\nu_8 - \nu_7) + \nu_8 \bar{x}_3^h},
\end{aligned}$$

and $\bar{x}_3$ is the unique solution to the equation

$$P_L(x_3) = P_R(x_3), \tag{14}$$

with

$$P_L(x_3) = \frac{k_1^n[k_7^h \nu_1(\nu_8 - \nu_7) + k_7^h k_8 \nu_7 \nu_c + \nu_1 \nu_8 x_3^h]}{(k_1^n + x_3^n)[k_7^h(\nu_8 - \nu_7) + \nu_8 x_3^h]}, \tag{15}$$

$$\begin{aligned}
P_R(x_3) = {} & \{[\nu_2\nu_6(\nu_4 + k_4\nu_5 + \nu_6)]x_3^2 + k_6\nu_2\nu_6(\nu_4 + k_4\nu_5)x_3\} \\
& \cdot \{[k_2\nu_3(k_4\nu_5 + \nu_6) + \nu_6(\nu_4 + k_4\nu_5 + \nu_6)]x_3^2 \\
& + [k_6(\nu_6(\nu_4 + k_4\nu_5) + k_2\nu_3(2k_4\nu_5 + \nu_6))]x_3 + k_2k_4k_6^2\nu_3\nu_5\}^{-1}.
\end{aligned} \tag{16}$$

Proof $(\bar{x}_1, \bar{x}_2, \bar{x}_3, \bar{x}_4, \bar{x}_1, \bar{x}_2, \bar{x}_3, \bar{x}_4)$ is a synchronous equilibrium for (9) if and only if $(x_1, x_2, x_3, x_4) = (\bar{x}_1, \bar{x}_2, \bar{x}_3, \bar{x}_4)$ satisfies

$$\begin{cases}
g_H(x_3, x_4) - f_1(x_1) = 0 \\
\nu_3 x_1 - f_2(x_2) = 0 \\
\nu_5 x_2 - f_3(x_3) = 0 \\
g_D(x_3) - f_4(x_4) = 0.
\end{cases}$$

Accordingly,

$$\begin{aligned}
\bar{x}_1 &= \frac{\nu_6\bar{x}_3(k_6(\nu_4+k_4\nu_5)+(\nu_4+k_4\nu_5+\nu_6)\bar{x}_3)}{\nu_3(k_6+\bar{x}_3)(\nu_6\bar{x}_3+k_4\nu_5(k_6+\bar{x}_3))},\\
\bar{x}_2 &= \frac{\nu_6\bar{x}_3}{\nu_5(k_6+\bar{x}_3)},\\
\bar{x}_4 &= \frac{k_7^h k_8\nu_7}{k_7^h(\nu_8-\nu_7)+\nu_8\bar{x}_3^h},
\end{aligned}$$

and $\bar{x}_3$ satisfies (14). Observe that there exists exactly one positive solution to (14), due to $\nu_8 > \nu_7$, and

$$\begin{aligned}
&P_R(0) = 0,\ \ P_R'(x_3) > 0,\ \text{for all } x_3 \geq 0,\\
&P_L(0) > 0,\ \ P_L'(x_3) < 0,\ \text{for all } x_3 > 0,
\end{aligned}$$

and

$$\begin{aligned}
&\lim_{x_3\to\infty} P_R(x_3) = \frac{\nu_2\nu_6(\nu_4+k_4\nu_5+\nu_6)}{k_2\nu_3(k_4\nu_5+\nu_6)+\nu_6(\nu_4+k_4\nu_5+\nu_6)} > 0,\\
&\lim_{x_3\to\infty} P_L(x_3) = 0.
\end{aligned}$$

Note that every component of $\bar{\mathbb{X}}$ is positive. The assertion thus follows. □

Now, let us discuss the global convergence to the synchronous equilibrium point $\bar{\mathbb{X}}$ for system (9). For simplicity, we change Q_i to $[0, \hat{q}_i]$, i.e., we take $\check{q}_i = 0$, for $i = 1, \ldots, 4$. First, we translate the equilibrium $\bar{\mathbb{X}}$ to the origin, i.e., we let $\tilde{\mathbf{x}}(t) = \mathbf{x}(t) - \bar{\mathbf{x}}$, $\tilde{\mathbf{y}}(t) = \mathbf{y}(t) - \bar{\mathbf{x}}$, and still denote $\tilde{\mathbf{x}}$, $\tilde{\mathbf{y}}$ by $\mathbf{x}$, $\mathbf{y}$, respectively. System (9) becomes

$$\begin{cases}
\dot{x}_1(t) = g_H(x_3(t-\tau_1)+\bar{x}_3, y_4(t-\tau_1)+\bar{x}_4) - f_1(x_1(t)+\bar{x}_1)\\
\dot{x}_2(t) = \nu_3[x_1(t-\tau_2)+\bar{x}_1] - f_2(x_2(t)+\bar{x}_2)\\
\dot{x}_3(t) = \nu_5[x_2(t)+\bar{x}_2] - f_3(x_3(t)+\bar{x}_3)\\
\dot{x}_4(t) = g_D(x_3(t-\tau_4)+\bar{x}_3) - f_4(x_4(t)+\bar{x}_4)\\
\dot{y}_1(t) = g_H(y_3(t-\tau_1)+\bar{x}_3, x_4(t-\tau_1)+\bar{x}_4) - f_1(y_1(t)+\bar{x}_1)\\
\dot{y}_2(t) = \nu_3[y_1(t-\tau_2)+\bar{x}_1] - f_2(y_2(t)+\bar{x}_2)\\
\dot{y}_3(t) = \nu_5[y_2(t)+\bar{x}_2] - f_3(y_3(t)+\bar{x}_3)\\
\dot{y}_4(t) = g_D(y_3(t-\tau_4)+\bar{x}_3) - f_4(y_4(t)+\bar{x}_4).
\end{cases} \tag{17}$$

We shall derive a criterion for global convergence to the origin in system (17). Let $\mathbb{X}(t) = (x_1(t), \ldots, x_4(t), y_1(t), \ldots, y_4(t))$ be an arbitrary solution of (17), which exists on $[0, \infty)$, according to Proposition 2. With $x_i(t)$, $y_i(t)$ satisfying (17), by mean value theorem, we obtain

$$\begin{cases}
\dot{x}_i(t) = -f_i'(\zeta_i(t))x_i(t) + w_i(t)\\
\dot{y}_i(t) = -f_i'(\zeta_{i+4}(t))y_i(t) + w_{i+4}(t),
\end{cases} \tag{18}$$

where $\zeta_i(t)$ (resp., $\zeta_{i+4}(t)$) is between $x_i(t)+\bar{x}_i$ and $\bar{x}_i$ (resp., $y_i(t)+\bar{x}_i$ and $\bar{x}_i$), $i=1,\ldots,4$, for all t large enough and

$$\begin{aligned}
w_1(t) &:= \frac{\partial g_H}{\partial u}(u_1(t-\tau_1), v_1(t-\tau_1))x_3(t-\tau_1)\\
&\quad + \frac{\partial g_H}{\partial v}(u_1(t-\tau_1), v_1(t-\tau_1))y_4(t-\tau_1),\\
w_2(t) &:= \nu_3 x_1(t-\tau_2),\\
w_3(t) &:= \nu_5 x_2(t),\\
w_4(t) &:= g_D'(u_4(t-\tau_4))x_3(t-\tau_4),\\
w_5(t) &:= \frac{\partial g_H}{\partial u}(\tilde{u}_1(t-\tau_1), \tilde{v}_1(t-\tau_1))y_3(t-\tau_1)\\
&\quad + \frac{\partial g_H}{\partial v}(\tilde{u}_1(t-\tau_1), \tilde{v}_1(t-\tau_1))x_4(t-\tau_1),\\
w_6(t) &:= \nu_3 y_1(t-\tau_2),\\
w_7(t) &:= \nu_5 y_2(t),\\
w_8(t) &:= g_D'(\tilde{u}_4(t-\tau_4))y_3(t-\tau_4),
\end{aligned}$$

where $u_1(t-\tau_1)$ (resp., $v_1(t-\tau_1), u_4(t-\tau_4), \tilde{u}_1(t-\tau_1), \tilde{v}_1(t-\tau_1), \tilde{u}_4(t-\tau_4)$) is some quantity between $x_3(t-\tau_1)+\bar{x}_3$ and $\bar{x}_3$ (resp., $y_4(t-\tau_1)+\bar{x}_4$ and $\bar{x}_4$, $x_3(t-\tau_4)+\bar{x}_3$ and $\bar{x}_3$, $y_3(t-\tau_1)+\bar{x}_3$ and $\bar{x}_3$, $x_4(t-\tau_1)+\bar{x}_4$ and $\bar{x}_4$, $y_3(t-\tau_4)+\bar{x}_3$ and $\bar{x}_3$). Note that $\mathbb{X}(t)$ converges to $\mathscr{Q}-\bar{\mathbb{X}} = \Pi_{i=1}^4 Q_i^* \times \Pi_{i=1}^4 Q_i^*$, where $Q_i^* := [\check{q}_i - \bar{x}_i, \hat{q}_i - \bar{x}_i]$, $i=1,\ldots,4$. Obviously, every component of (18) takes the form

$$\dot{v}(t) = -f'(\zeta(t))v(t) + w(t), \tag{19}$$

where $\zeta(t)$ lies in a compact set $\tilde{Q}$ for all t large enough and $w(t)$ is a continuous scalar function. We denote

$$\begin{aligned}
|w|^{\max}(t) &:= \sup\{|w(s)| : s \geq t\}, \text{ for } t \geq 0\\
|w|^{\max}(\infty) &:= \lim_{t\to\infty} |w|^{\max}(t),\\
\check{d} &:= \min\{f'(\zeta) : \zeta \in \tilde{Q}\}.
\end{aligned}$$

It is straightforward to derive the following lemma; cf. Shih and Tseng (2008).

Lemma 1 *Every solution of (19) converges to an interval* $[-\tilde{\delta}, \tilde{\delta}]$ *as* $t \to \infty$, *where*

$$0 \leq \tilde{\delta} \leq |w|^{\max}(\infty)/\check{d}.$$

From Lemma 1, there exist eight intervals $I_i := [-\delta_i, \delta_i]$, $i=1,\ldots,8$, to which the ith component of solution $\mathbb{X}(t)$ of (18) converges respectively. Since $\zeta_i(t), \zeta_{i+4}(t) \in Q_i$ for all t large enough, we obtain

$$0 \le \delta_i \le |w_i|^{\max}(\infty)/\check{d}_i, \text{ for } i = 1, \ldots, 4,$$
$$0 \le \delta_i \le |w_i|^{\max}(\infty)/\check{d}_{i-4}, \text{ for } i = 5, \ldots, 8,$$

where

$$\begin{aligned}
\check{d}_1 &:= \min\{f_1'(\zeta_1) : \zeta_1 \in Q_1\} = \frac{k_2 \nu_2}{(k_2 + \hat{q}_1)^2}, \\
\check{d}_2 &:= \min\{f_2'(\zeta_2) : \zeta_2 \in Q_2\} = \frac{k_4 \nu_4}{(k_4 + \hat{q}_2)^2} + \nu_5, \\
\check{d}_3 &:= \min\{f_3'(\zeta_3) : \zeta_3 \in Q_3\} = \frac{k_6 \nu_6}{(k_6 + \hat{q}_3)^2}, \\
\check{d}_4 &:= \min\{f_4'(\zeta_4) : \zeta_4 \in Q_4\} = \frac{k_8 \nu_8}{(k_8 + \hat{q}_4)^2}.
\end{aligned} \tag{20}$$

Next, we shall estimate the value of δ_i through an iterative process. First, we define

$$\begin{aligned}
\rho_1 &:= \max\left\{\left|\frac{\partial g_H(u, v)}{\partial u}\right| : u \in Q_3, v \in Q_4\right\}, \\
\rho_2 &:= \max\left\{\left|\frac{\partial g_H(u, v)}{\partial v}\right| : u \in Q_3, v \in Q_4\right\}, \\
\rho_3 &:= \max\{|g_D'(u)| : u \in Q_3\}.
\end{aligned} \tag{21}$$

Proposition 4 *For each $i = 1, \ldots, 8$, there exists a sequence of nonnegative numbers $\{\delta_i^{(k)}\}_{k=1}^{\infty}$ with $\delta_i^{(k)} \ge \delta_i$ such that for each k, the ith component for the solution $\mathbb{X}(t)$ of system (17) converges to $I_i^{(k)} := [-\delta_i^{(k)}, \delta_i^{(k)}]$, as $t \to \infty$, and $\delta_i^{(k)}$ satisfies*

$$\begin{aligned}
0 \le \delta_1^{(k)} = \delta_5^{(k)} &:= \left(\rho_1 \delta_3^{(k-1)} + \rho_2 \delta_4^{(k-1)}\right)/\check{d}_1, \\
0 \le \delta_2^{(k)} = \delta_6^{(k)} &:= (\nu_3/\check{d}_2)\delta_1^{(k)}, \\
0 \le \delta_3^{(k)} = \delta_7^{(k)} &:= (\nu_5/\check{d}_3)\delta_2^{(k)}, \\
0 \le \delta_4^{(k)} = \delta_8^{(k)} &:= (\rho_3/\check{d}_4)\delta_3^{(k)},
\end{aligned} \tag{22}$$

where $k \ge 1$, $\delta_3^{(0)} := \max\{|\check{q}_3 - \bar{x}_3|, |\hat{q}_3 - \bar{x}_3|\}$, $\delta_4^{(0)} := \max\{|\check{q}_4 - \bar{x}_4|, |\hat{q}_4 - \bar{x}_4|\}$, and ρ_i is defined in (21).

The proof is similar to the one for Proposition 2.5 in Liao et al. (2012) and is omitted.

Theorem 1 *Every solution of system (9) converges to the synchronous equilibrium point $\bar{\mathbb{X}}$ as $t \to \infty$, if*

$$\nu_3 \nu_5 (\rho_1 \check{d}_4 + \rho_2 \rho_3) < \check{d}_1 \check{d}_2 \check{d}_3 \check{d}_4. \tag{23}$$

Proof To justify the assertion, we shall prove that every solution of (18) converges to the origin, as $t \to \infty$. It suffices to show that $\delta_i^{(k)}$ introduced in Proposition 4 converges to zero as k tends to infinity, for all $i = 1, \ldots, 8$. From (22), we obtain

$$\begin{aligned}
\delta_1^{(k)} &= \left(\rho_1 \delta_3^{(k-1)} + \rho_2 \delta_4^{(k-1)}\right) / \check{d}_1 \\
&= \frac{\rho_1 \nu_3 \nu_5}{\check{d}_1 \check{d}_2 \check{d}_3} \delta_1^{(k-1)} + \frac{\rho_2 \nu_3 \nu_5 \rho_3}{\check{d}_1 \check{d}_2 \check{d}_3 \check{d}_4} \delta_1^{(k-1)} \\
&= \frac{\nu_3 \nu_5 (\rho_1 \check{d}_4 + \rho_2 \rho_3)}{\check{d}_1 \check{d}_2 \check{d}_3 \check{d}_4} \delta_1^{(k-1)} \\
&=: \mathscr{R} \delta_1^{(k-1)}.
\end{aligned}$$

Thus $\delta_1^{(k)} \to 0$, as $k \to \infty$, since $0 < \mathscr{R} < 1$, by (23). Subsequently, $\delta_i^{(k)} \to 0$, as $k \to \infty$, for $i = 2, \ldots, 8$, according to (22). □

Remark 2 (i) In fact, the upper bounds for the derivatives of g_H and g_D can be computed as

$$\begin{aligned}
0 \le \left| \frac{\partial g_H(u, v)}{\partial u} \right| &\le \frac{n(\nu_1 + \nu_c \hat{q}_4) \hat{q}_3^{n-1}}{k_1^n} =: \hat{\rho}_1, \ \text{for } u \in Q_3, v \in Q_4, \\
0 \le \left| \frac{\partial g_H(u, v)}{\partial v} \right| &\le \nu_c =: \hat{\rho}_2, \ \text{for } u \in Q_3, v \in Q_4, \\
0 \le |g_D'(u)| &\le \frac{h \nu_7 \hat{q}_3^{h-1}}{k_7^h} =: \hat{\rho}_3, \ \text{for } u \in Q_3.
\end{aligned} \tag{24}$$

Note that $\hat{\rho}_i$ is computable and $\hat{\rho}_i \ge \rho_i$, $i = 1, 2, 3$. Therefore, condition (23) can be replaced by an explicit inequality:

$$\nu_3 \nu_5 (\hat{\rho}_1 \check{d}_4 + \hat{\rho}_2 \hat{\rho}_3) < \check{d}_1 \check{d}_2 \check{d}_3 \check{d}_4. \tag{25}$$

(ii) By Theorem 1, $\bar{\mathbb{X}}$ is a unique equilibrium for system (9) under (23) or (25).

Since all solutions tend to a steady state, the parameter regime under (23) or (25) corresponds to the non-oscillatory or oscillation-arrested phase for model (9), which is associated with the state of formed somites. Moreover, under condition (23) or (25), the magnitude of each $\bar{x}_i$ determines the ultimate behavior of the system. In the following proposition, we further discuss how the parameters affect the magnitude of $\bar{x}_i$, for $i = 1, \ldots, 4$.

Proposition 5 *$\bar{x}_4$ increases and $\bar{x}_i$, $i = 1, 2, 3$, decreases, as one of k_1, k_2, ν_1, ν_c decreases or ν_2 increases.*

Proof From (16), we see that if k_2 decreases or ν_2 increases, then $P_R(x_3)$ increases and $P_L(x_3)$ is unchanged, and thus $\bar{x}_3$ decreases. Similarly, if k_1, ν_1, or ν_c decreases, then $P_L(x_3)$ decreases and $P_R(x_3)$ is unchanged, and therefore $\bar{x}_3$ decreases. The assertions follow from $\frac{\partial}{\partial \bar{x}_3} \bar{x}_1 > 0$, $\frac{\partial}{\partial \bar{x}_3} \bar{x}_2 > 0$, and $\frac{\partial}{\partial \bar{x}_3} \bar{x}_4 < 0$. □

Proposition 5 indicates that if the transcription rate of *her* mRNA decreases or the degradation rate of *her* mRNA increases, then the steady state of *her* mRNA, Her protein, and *delta* mRNA all decrease and the Delta protein increases.

All the results in this section hold for $\tau_1 = \tau_2 = \tau_4 = 0$, i.e., the ODE system (8) proposed in Uriu et al. (2010). The discussions herein can be extended to transcription functions g_H and g_D in more general form with $\frac{\partial}{\partial u} g_H(u, v) < 0$, $\frac{\partial}{\partial v} g_H(u, v) > 0$, and $\frac{d}{du} g_D(u) < 0$, for all $u, v \geq 0$.

4 Synchronous oscillations

To elucidate synchronous oscillations through cell–cell interaction in segmentation clocks, we study synchronous periodic solutions generated in systems (8) and (9). In Sect. 4.1, for the ODE system (8), we take one of the activation parameters as bifurcation parameter and employ Hopf bifurcation theory to analyze the existence and stability of periodic solutions. In Sect. 4.2, we fix suitable values of all parameters in the delay system (9), and use the sum of transcription delay and translation delay as bifurcation parameter to apply the delay Hopf bifurcation theory. It will be seen that synchronous periodic solutions with periods around 30 min exist in each of these two systems, at certain parameter values.

4.1 ODE model (8)

We study the ODE model (8) with transcription function (6) and degradations (7). We plan to investigate the periodic solutions bifurcating from the synchronous equilibrium $\bar{\mathbb{X}} = (\bar{\mathbf{x}}, \bar{\mathbf{x}})$, with $\bar{\mathbf{x}} = (\bar{x}_1, \bar{x}_2, \bar{x}_3, \bar{x}_4)$, of this system via Hopf bifurcation theorem. Let $\tilde{\mathbf{x}}(t) = \mathbf{x}(t) - \bar{\mathbf{x}}$, $\tilde{\mathbf{y}}(t) = \mathbf{y}(t) - \bar{\mathbf{x}}$, and still denote $\tilde{\mathbf{x}}$, $\tilde{\mathbf{y}}$ by $\mathbf{x}$, $\mathbf{y}$ respectively. The system becomes

$$
\begin{cases}
\dot{x}_1 = \dfrac{k_1^n}{k_1^n + (x_3 + \bar{x}_3)^n}[\nu_1 + \nu_c(y_4 + \bar{x}_4)] - \dfrac{\nu_2(x_1 + \bar{x}_1)}{k_2 + (x_1 + \bar{x}_1)} \\
\dot{x}_2 = \nu_3(x_1 + \bar{x}_1) - \dfrac{\nu_4(x_2 + \bar{x}_2)}{k_4 + (x_2 + \bar{x}_2)} - \nu_5(x_2 + \bar{x}_2) \\
\dot{x}_3 = \nu_5(x_2 + \bar{x}_2) - \dfrac{\nu_6(x_3 + \bar{x}_3)}{k_6 + (x_3 + \bar{x}_3)} \\
\dot{x}_4 = \dfrac{\nu_7 k_7^h}{k_7^h + (x_3 + \bar{x}_3)^h} - \dfrac{\nu_8(x_4 + \bar{x}_4)}{k_8 + (x_4 + \bar{x}_4)} \\
\dot{y}_1 = \dfrac{k_1^n}{k_1^n + (y_3 + \bar{x}_3)^n}[\nu_1 + \nu_c(x_4 + \bar{x}_4)] - \dfrac{\nu_2(y_1 + \bar{x}_1)}{k_2 + (y_1 + \bar{x}_1)} \\
\dot{y}_2 = \nu_3(y_1 + \bar{x}_1) - \dfrac{\nu_4(y_2 + \bar{x}_2)}{k_4 + (y_2 + \bar{x}_2)} - \nu_5(y_2 + \bar{x}_2) \\
\dot{y}_3 = \nu_5(y_2 + \bar{x}_2) - \dfrac{\nu_6(y_3 + \bar{x}_3)}{k_6 + (y_3 + \bar{x}_3)} \\
\dot{y}_4 = \dfrac{\nu_7 k_7^h}{k_7^h + (y_3 + \bar{x}_3)^h} - \dfrac{\nu_8(y_4 + \bar{x}_4)}{k_8 + (y_4 + \bar{x}_4)}.
\end{cases}
\tag{26}
$$

The linearization of system (26) at the origin is given by

$$\begin{cases} \dot{u}_1 = -\dfrac{\nu_2 k_2}{(k_2+\bar{x}_1)^2}u_1 - \dfrac{k_1^n n \bar{x}_3^{n-1}(\nu_1+\nu_c\bar{x}_4)}{(k_1^n+\bar{x}_3^n)^2}u_3 + \dfrac{\nu_c k_1^n}{(k_1^n+\bar{x}_3^n)}v_4 \\ \dot{u}_2 = \nu_3 u_1 - \left(\dfrac{\nu_4 k_4}{(k_4+\bar{x}_2)^2}+\nu_5\right)u_2 \\ \dot{u}_3 = \nu_5 u_2 - \dfrac{\nu_6 k_6}{(k_6+\bar{x}_3)^2}u_3 \\ \dot{u}_4 = -\dfrac{k_7^h h \bar{x}_3^{h-1}\nu_7}{(k_7^h+\bar{x}_3^h)^2}u_3 - \dfrac{\nu_8 k_8}{(k_8+\bar{x}_4)^2}u_4 \\ \dot{v}_1 = -\dfrac{\nu_2 k_2}{(k_2+\bar{x}_1)^2}v_1 - \dfrac{k_1^n n \bar{x}_3^{n-1}(\nu_1+\nu_c\bar{x}_3)}{(k_1^n+\bar{x}_3^n)^2}v_3 + \dfrac{\nu_c k_1^n}{(k_1^n+\bar{x}_3^n)}u_4 \\ \dot{v}_2 = \nu_3 v_1 - \left(\dfrac{\nu_4 k_4}{(k_4+\bar{x}_2)^2}+\nu_5\right)v_2 \\ \dot{v}_3 = \nu_5 v_2 - \dfrac{\nu_6 k_6}{(k_6+\bar{x}_3)^2}v_3 \\ \dot{v}_4 = -\dfrac{\nu_7 k_7^h h \bar{x}_3^{h-1}}{(k_7^h+\bar{x}_3^h)^2}v_3 - \dfrac{\nu_8 k_8}{(k_8+\bar{x}_4)^2}v_4. \end{cases} \tag{27}$$

The characteristic equation for (27) is $\Delta = 0$, where

$$\Delta = \det\begin{pmatrix} \lambda+d_1 & 0 & \gamma_1 & 0 & 0 & 0 & 0 & -\gamma_2 \\ -\nu_3 & \lambda+d_2 & 0 & 0 & 0 & 0 & 0 & 0 \\ 0 & -\nu_5 & \lambda+d_3 & 0 & 0 & 0 & 0 & 0 \\ 0 & 0 & \gamma_3 & \lambda+d_4 & 0 & 0 & 0 & 0 \\ 0 & 0 & 0 & -\gamma_2 & \lambda+d_1 & 0 & \gamma_1 & 0 \\ 0 & 0 & 0 & 0 & -\nu_3 & \lambda+d_2 & 0 & 0 \\ 0 & 0 & 0 & 0 & 0 & -\nu_5 & \lambda+d_3 & 0 \\ 0 & 0 & 0 & 0 & 0 & 0 & \gamma_3 & \lambda+d_4 \end{pmatrix},$$

and

$$\begin{aligned} d_1 &:= \frac{\nu_2 k_2}{(k_2+\bar{x}_1)^2},\ d_2 := \frac{\nu_4 k_4}{(k_4+\bar{x}_2)^2}+\nu_5, \\ d_3 &:= \frac{\nu_6 k_6}{(k_6+\bar{x}_3)^2},\ d_4 := \frac{\nu_8 k_8}{(k_8+\bar{x}_4)^2}, \\ \gamma_1 &:= \frac{k_1^n n \bar{x}_3^{n-1}}{(k_1^n+\bar{x}_3^n)^2}(\nu_1+\nu_c\bar{x}_4), \\ \gamma_2 &:= \frac{\nu_c k_1^n}{k_1^n+\bar{x}_3^n}, \\ \gamma_3 &:= \frac{\nu_7 k_7^h h \bar{x}_3^{h-1}}{(k_7^h+\bar{x}_3^h)^2}. \end{aligned} \tag{28}$$

(29)

The characteristic equation $\Delta = 0$ can be factored as

$$\Delta_+ \cdot \Delta_- = 0, \tag{30}$$

where

$$\begin{aligned}
\Delta_\pm &= \lambda^4 + \beta_1\lambda^3 + \beta_2\lambda^2 + \beta_3\lambda + \beta_4 + \nu_3\nu_5\gamma_1\lambda + \nu_3\nu_5(d_4\gamma_1 \pm \gamma_2\gamma_3),\\
\beta_1 &:= d_1 + d_2 + d_3 + d_3 > 0,\\
\beta_2 &:= d_3d_4 + d_1(d_2 + d_3 + d_4) + d_2(d_3 + d_4) > 0,\\
\beta_3 &:= d_2d_3(d_1 + d_4) + d_1d_4(d_2 + d_3) > 0,\\
\beta_4 &:= d_1d_2d_3d_4 > 0.
\end{aligned} \tag{31}$$

Then, by the Routh–Hurwitz criterion, all roots of (30) have negative real parts if and only if

$$\alpha_1 > 0, \alpha_3 > 0, \alpha_4^\pm > 0,\ \alpha_1\alpha_2\alpha_3 - \alpha_3^2 - \alpha_3^2\alpha_4^\pm > 0, \tag{32}$$

where $\alpha_1 := \beta_1, \alpha_2 := \beta_2, \alpha_3 := \beta_3 + \nu_3\nu_5\gamma_1, \alpha_4^\pm := \beta_4 + \nu_3\nu_5(d_4\gamma_1 \pm \gamma_2\gamma_3)$. As $\alpha_1, \alpha_3, \alpha_4^+ > 0$, and $\alpha_4^+ > \alpha_4^-$, condition (32) reduces to

$$\alpha_4^- > 0,\ \ \alpha_1\alpha_2\alpha_3 - \alpha_3^2 - \alpha_3^2\alpha_4^+ > 0, \tag{33}$$

$$\text{or } \alpha_4^- > 0,\ \ \nu_3\nu_5(\gamma_2\gamma_3 - d_4\gamma_1) < \beta_4 < \frac{\alpha_1\alpha_2\alpha_3 - \alpha_3^2}{\alpha_1^2} - \nu_3\nu_5(d_4\gamma_1 + \gamma_2\gamma_3). \tag{34}$$

Lemma 2 *All roots of* (30) *have negative real parts if and only if* (33) *or* (34) *holds.*

In fact, Routh–Hurwitz criterion leads to the condition under which a pair of purely imaginary eigenvalues exist, while the rest of eigenvalues still have negative real parts (Asada and Yoshida 2003). The following lemma can thus be derived.

Lemma 3 *The equation $\Delta_+ = 0$ (resp., $\Delta_- = 0$) has a pair of purely imaginary roots, and its remaining roots have negative real parts if and only if*

$$\begin{aligned}
&\alpha_1 > 0, \alpha_3 > 0, \alpha_4^+ > 0,\ \ \textit{and}\ \alpha_1\alpha_2\alpha_3 - \alpha_3^2 - \alpha_1^2\alpha_4^+ = 0,\\
&(resp.,)\ \alpha_1 > 0, \alpha_3 > 0, \alpha_4^- > 0,\ \ \textit{and}\ \alpha_1\alpha_2\alpha_3 - \alpha_3^2 - \alpha_1^2\alpha_4^- = 0.
\end{aligned}$$

The following proposition follows from (32) and Lemma 3, and $\alpha_1 > 0, \alpha_3 > 0, \alpha_4^+ > 0$, and $\alpha_4^+ > \alpha_4^-$.

Proposition 6 *The equation $\Delta = 0$ has a pair of purely imaginary roots and the remaining roots have negative real parts if and only if $\alpha_4^- > 0$ and*

$$\alpha_1\alpha_2\alpha_3 - \alpha_3^2 - \alpha_1^2\alpha_4^+ = 0. \tag{35}$$

Notably, this pair of purely imaginary roots are roots of $\Delta_+ = 0$, and (35) is equivalent to

$$\beta_4 = \frac{\alpha_1\alpha_2\alpha_3 - \alpha_3^2}{\alpha_1^2} - \nu_3\nu_5(d_4\gamma_1 + \gamma_2\gamma_3).$$

To apply the Hopf bifurcation theorem, one first need to find a set of parameter values at which a pair of eigenvalues cross the imaginary axis of complex plane transversally and real parts of the other eigenvalues remain negative. We denote by μ one of the parameters in (8) and fix the other parameters, while allow μ to vary. The synchronous equilibrium $\bar{\mathbb{X}}$, and hence the characteristic roots of (30) then depend on μ. We thus obtain the following Hopf bifurcation theorem.

Theorem 2 *Consider system* (8) *which has a synchronous equilibrium* $\bar{\mathbb{X}}$ *at certain fixed parameters and* $\mu = \mu^*$. *Assume that the synchronous equilibrium is a function of* μ *for* μ *near* μ^*, *i.e.,* $\bar{\mathbb{X}} = \bar{\mathbb{X}}(\mu)$, *and*

$$\begin{aligned}
&\alpha_4^-(\mu^*) > 0\\
&\alpha_1(\mu^*)\alpha_2(\mu^*)\alpha_3(\mu^*) - \alpha_3^2(\mu^*) - \alpha_1^2(\mu^*)\alpha_4^+(\mu^*) = 0,\\
&\frac{d}{d\mu}[\alpha_1(\mu)\alpha_2(\mu)\alpha_3(\mu) - \alpha_3^2(\mu) - \alpha_1^2(\mu)\alpha_4^+(\mu)]|_{\mu=\mu^*} \neq 0,
\end{aligned} \tag{36}$$

where the coefficients $\alpha_i = \alpha_i(\mu)$, $i = 1, 2, 3$, *and* $\alpha_4^{\pm} = \alpha_4^{\pm}(\mu)$ *of* $\Delta_\pm$ *are functions of* μ. *Then the system undergoes a Hopf bifurcation at* $\mathbb{X} = \bar{\mathbb{X}}$ *and* $\mu = \mu^*$, *and a small-amplitude synchronous periodic solution surrounding* $\bar{\mathbb{X}}$ *emerges as* $\mu < \mu^*$ *or* $\mu > \mu^*$ *and* μ *is close to* μ^*.

The proof of this theorem is sketched in "Appendix 1". Notably, the assumption that the synchronous equilibrium is a function of μ for μ near μ^* can be realized by the implicit function theorem. System (8) consists of two identical cells under symmetric coupling, and thus $S := \{x_1 = y_1, x_2 = y_2, x_3 = y_3, x_4 = y_4\}$ is positively invariant under the solution flow. The characteristic equation restricted to S is exactly $\Delta_+ = 0$. Therefore, Theorem 2 leads to the existence of synchronous periodic solution. We can transform the system into normal form, and apply the center manifold theorem to analyze the stability of the bifurcating periodic solution. We summarize these formulations in "Appendix 2", following the theory in Hassard et al. (1981). From the formulations, we obtain the following qualities

$$\begin{aligned}
C_1(\mu^*) &= \frac{i}{2\omega_0}\left(g_{20}g_{11} - 2|g_{11}|^2 - \frac{1}{3}|g_{02}|^2\right) + \frac{g_{21}}{2},\\
p_2 &= -\frac{\mathrm{Re}(C_1(\mu^*))}{\mathrm{Re}(\lambda'(\mu^*))},\\
\zeta_2 &= 2\mathrm{Re}(C_1(\mu^*)),\\
T_2 &= \frac{-1}{\omega_0}[\mathrm{Im}(C_1(\mu^*)) + p_2\mathrm{Im}(\lambda'(\mu^*))],
\end{aligned}$$

where $\lambda(\mu)$ is the eigenvalue crossing the imaginary axis at $\mu = \mu^*$, $\lambda(\mu^*) = i\omega_0$, and $g_{20}, g_{11}, g_{02}, g_{21}$ are defined in "Appendix 2". These quantities can be computed numerically for the application of the following Hopf bifurcation theorem, recast from Hassard et al. (1981).

Theorem 3 *Under the conditions of Theorem 2, the following hold for system (8):*

(i) *The Hopf bifurcation is supercritical (resp., subcritical) and a bifurcating periodic solution exists for $\mu > \mu^*$ (resp., $\mu < \mu^*$) with μ near μ^*, if $p_2 > 0$ (resp., < 0).*
(ii) *The periodic solution is stable (resp., unstable), if $\zeta_2 < 0$ (resp., > 0).*
(iii) *The period increases (resp., decreases) as μ increases, if $T_2 > 0$ (resp., < 0) and $p_2 > 0$; the period increases (resp., decreases) as μ decreases, if $T_2 < 0$ (resp., > 0) and $p_2 < 0$.*

Performing bifurcation analysis in an ODE system with more than a dozen of parameters, such as (8), appears to be a difficult task, as commented in Uriu et al. (2010). One complication is that the equilibrium depends on the parameters, and thus the linearization at the equilibrium varies with parameter values in an implicit way. Nevertheless, our formulation above indicates that the Hopf bifurcation analysis still can be carried out, if we combine the Routh–Hurwitz criterion with numerical computation effectively. Let us demonstrate such analysis and computation in the following examples.

4.1.1 Numerical illustrations

In the following examples, we adopt the parameter values in Uriu et al. (2010) and illustrate that the numerically computed synchronous oscillation therein is generated by the Hopf bifurcation presented in Theorem 2. Zebrafish segmentation clock is around 30 min, and thus we focus on periodic solutions with periods within [25, 35] min. We take $\mu = \nu_7$ and $\mu = \nu_c$ as the bifurcation parameter in Examples 4.1 and 4.2, respectively. In Example 4.3, we show that the single-cell (decoupled-cell) system, i.e., system (8) with $\nu_c = 0$, does not admit periodic solution when the coupled-cell system does. In Example 4.4, we illustrate the dynamical disparity between a system with linear degradations and a system with Michaelis–Menten degradations.

Example 4.1 We choose $\mu = \nu_7$, the synthesis rate of Delta protein, as the bifurcation parameter. The values of the other parameters are adopted from Uriu et al. (2010), and shown in Tables 1 and 2. Note that ν_7 appears in γ_3 in the characteristic equation (30). Thus, we single out ν_7 from γ_3 by setting

$$\gamma_3 = \nu_7 \tilde{\gamma}_3, \text{ with } \tilde{\gamma}_3 := \frac{k_7^h h \bar{x}_3^{h-1}}{(k_7^h + \bar{x}_3^h)^2},$$

so that $\alpha_4^+ = \beta_4 + \nu_3\nu_5\nu_7\gamma_2\tilde{\gamma}_3$. We look for a value for ν_7 which satisfies

$$\alpha_1(\nu_7)\alpha_2(\nu_7)\alpha_3(\nu_7) - \alpha_3^2(\nu_7) - \alpha_1^2(\nu_7)\alpha_4^+(\nu_7) = 0.$$

Table 1 The parameter values of the transcription rate, translation rate, transportation rate and degradation rate in Uriu et al. (2010)

ν_c	ν_1	ν_2	ν_3	ν_4	ν_5	ν_6	ν_8
0.708	0.069	0.963	1.172	1.447	0.076	0.147	2.315

Table 2 The parameter values of the threshold constants and Michaelis constants in Uriu et al. (2010)

k_1	k_2	k_4	k_6	k_7	k_8	n	h
0.103	9.916	0.182	0.302	1.87	0.377	2	2

From this equality, ν_7 can be expressed by the other parameters and substituted into system (8) to solve the equilibrium. Here, the synchronous equilibrium of (8) with parameter values in Tables 1 and 2 can be computed as $\bar{\mathbb{X}} = (\bar{\mathbf{x}}, \bar{\mathbf{x}})$, with $\bar{\mathbf{x}} = (\bar{x}_1, \bar{x}_2, \bar{x}_3, \bar{x}_4)$, and $\bar{x}_1 \approx 1.040873, \bar{x}_2 \approx 0.745985, \bar{x}_3 \approx 0.189600, \bar{x}_4 \approx 0.469586$. With this value of $\bar{\mathbf{x}}$, we then compute to obtain the potential bifurcation value $\nu_7^* \approx 1.29729$. Next, we compute to find

$$\begin{aligned}
&\alpha_1(\nu_7^*) = 1.862781 > 0,\ \alpha_3(\nu_7^*) = 0.212131 > 0,\\
&\alpha_4^+(\nu_7^*) = 0.089593 > 0,\ \alpha_4^-(\nu_7^*) = 0.085631 > 0,\\
&\alpha_1(\nu_7^*)\alpha_2(\nu_7^*)\alpha_3(\nu_7^*) - \alpha_3^2(\nu_7^*) - \alpha_1^2(\nu_7^*)\alpha_4^-(\nu_7^*) = 0.013745 > 0,\\
&\frac{d}{d\nu_7}[\alpha_1(\nu_7)\alpha_2(\nu_7)\alpha_3(\nu_7) - \alpha_3^2(\nu_7) - \alpha_1^2(\nu_7)\alpha_4^+(\nu_7)]|_{\nu_7=\nu_7^*} = -0.005298 \neq 0.
\end{aligned}$$

Therefore, the conditions of Theorem 2 are met, and a small-amplitude periodic solution emerges, as the value of ν_7 passes through ν_7^*, according to Theorem 2. The solution evolved from initial value $\phi = (0.1, 0.1, 0.1, 0.1, 0.08, 0.08, 0.08, 0.08)$ is shown in Fig. 1. The periods and amplitudes of the oscillations corresponding to various values of ν_7 are listed in Fig. 2. We observe that the periods of oscillations increase as ν_7 increases. When $\nu_7 = 1.912$, the parameter value used in Uriu et al. (2010), this system generates a synchronous oscillation with period about 35 min.

Example 4.2 We choose $\mu = \nu_c$, the activation rate of *her* mRNA transcription by Delta–Notch signaling (the coupling strength), as the bifurcation parameter. The other parameter values are taken from Tables 1 and 2, except that $\nu_7 = 1.912$ is fixed and ν_c is varying. We single out ν_c from γ_1 and γ_2 by setting

$$\begin{aligned}
\gamma_1 &= (\nu_1 + \nu_c\bar{x}_4)\tilde{\gamma}_1, \text{ with } \tilde{\gamma}_1 := \frac{k_1^n n\bar{x}_3^{n-1}}{(k_1^n + \bar{x}_3^n)^2},\\
\gamma_2 &= \nu_c\tilde{\gamma}_2, \text{ with } \tilde{\gamma}_2 := \frac{k_1^n}{k_1^n + \bar{x}_3^n}.
\end{aligned}$$

Then α_3, α_4^+, and β_4 in the characteristic equation Δ_+ become

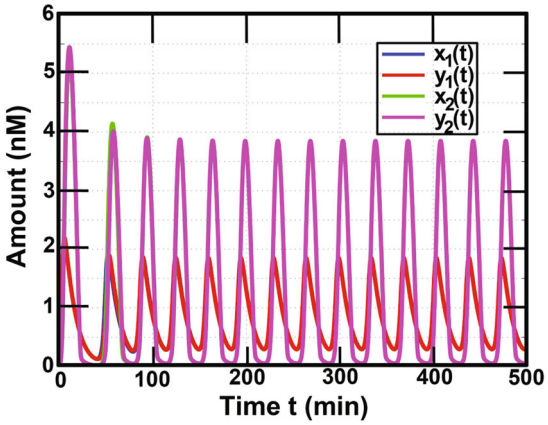

Fig. 1 Components x_1, y_1, x_2, y_2 of the solution of system (8), evolved from $\phi = (0.1, 0.1, 0.1, 0.1, 0.08, 0.08, 0.08, 0.08)$, with parameter values in Tables 1 and 2, and $\nu_7 = 1.912$. The solution converges toward a synchronous periodic solution

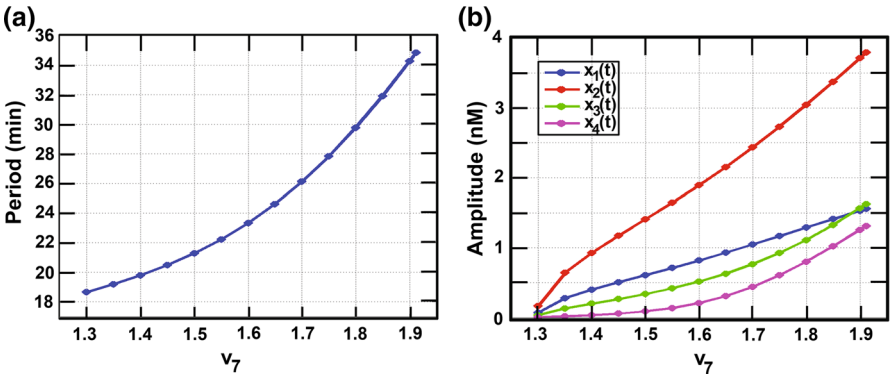

Fig. 2 The periods and amplitudes of the oscillations corresponding to various values of ν_7

$$\alpha_3 = \beta_3 + (\nu_1 + \nu_c \bar{x}_4)\nu_3\nu_5\tilde{\gamma}_1,$$
$$\alpha_4^+ = \beta_4 + (\nu_1 + \nu_c \bar{x}_4)\nu_3\nu_5 d_4\tilde{\gamma}_1 + \nu_3\nu_5\nu_c\tilde{\gamma}_2\gamma_3.$$

We look for a value of ν_c which satisfies

$$\alpha_1(\nu_c)\alpha_2(\nu_c)\alpha_3(\nu_c) - \alpha_3^2(\nu_c) - \alpha_1^2(\nu_c)\alpha_4^+(\nu_c) = 0.$$

By expressing ν_c in terms of the other parameters, we find the equilibrium $\bar{\mathbb{X}} = (\bar{\mathbf{x}}, \bar{\mathbf{x}})$, with $\bar{\mathbf{x}} = (\bar{x}_1, \bar{x}_2, \bar{x}_3, \bar{x}_4)$, and $\bar{x}_1 \approx 1.038105, \bar{x}_2 \approx 0.737551, \bar{x}_3 \approx 0.186135, \bar{x}_4 \approx 1.692328$, at which the bifurcation takes place. We then compute to find $\nu_c^* \approx 0.189266$, and

$$\alpha_1(\nu_c^*) = 0.857159 > 0,\ \alpha_3(\nu_c^*) = 0.096632 > 0,$$
$$\alpha_4^+(\nu_c^*) = 0.015588 > 0,\ \alpha_4^-(\nu_c^*) = 0.014011 > 0,$$
$$\alpha_1(\nu_c^*)\alpha_2(\nu_c^*)\alpha_3(\nu_c^*) - \alpha_3^2(\nu_c^*) - \alpha_1^2(\nu_c^*)\alpha_4^-(\nu_c^*) = 0.0011589 > 0,$$
$$\frac{d}{d\nu_c}[\alpha_1(\nu_c)\alpha_2(\nu_c)\alpha_3(\nu_c) - \alpha_3^2(\nu_c) - \alpha_1^2(\nu_c)\alpha_4^+(\nu_c)]|_{\nu_c=\nu_c^*} = -0.040228 \neq 0.$$

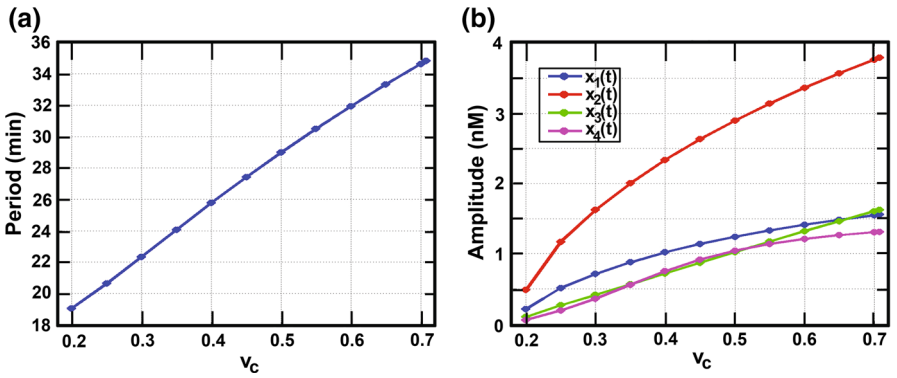

Fig. 3 The periods and amplitudes of the oscillations corresponding to various values of ν_c

Thus, as the value of ν_c passes through ν_c^*, there emerges a small-amplitude periodic solution which surrounds the synchronous equilibrium $\bar{\mathbb{X}}$. The periods and amplitudes of oscillations corresponding to various values of ν_c are listed in Fig. 3, and it appears that the period increases as ν_c increases. When $\nu_c = 0.708$, the system generates a synchronous oscillation, as in Example 4.1.

Example 4.3 Consider the single-cell or decoupled-cell system:

$$\begin{cases} \dot{x}_1(t) = g_H(x_3(t), 0) - f_1(x_1(t)) \\ \dot{x}_2(t) = \nu_3 x_1(t) - f_2(x_2(t)) \\ \dot{x}_3(t) = \nu_5 x_2(t) - f_3(x_3(t)) \\ \dot{x}_4(t) = g_D(x_3(t)) - f_4(x_4(t)), \end{cases} \tag{37}$$

i.e., system (8) with $\nu_c = 0$. First, we are interested in seeing whether such single-cell system (37) also admits a periodic solution with the parameter values in Tables 1 and 2, and $\nu_7 = 1.912$. We compute to find that, with these parameter values, the eigenvalues of the linearized system of (37) at the equilibrium $\bar{\mathbf{x}} = (\bar{x}_1, \bar{x}_2, \bar{x}_3, \bar{x}_4)$ all have negative real parts, where $\bar{x}_1 \approx 0.673668$, $\bar{x}_2 \approx 0.209108$, $\bar{x}_3 \approx 0.036607$, $\bar{x}_4 \approx 1.784716$. Numerical simulation shows that solutions originated from numerous initial values converge to the equilibrium $\bar{\mathbf{x}}$, as shown in Fig. 4. Hence, it appears that the single-cell system (37) does not generate periodic solution with these parameter values, whereas there is a synchronous oscillation in the coupled-cell system with the same parameter values and $\nu_c = 0.708$.

One is curious about whether if the single-cell system (37) can ever generate oscillation. By the Hopf bifurcation analysis, we observe that, with the parameter values in Tables 1 and 2, except now taking ν_1 near $\nu_1^* \approx 0.25209$, a small-amplitude periodic solution emerges, see Fig. 5. Note that ν_1 is considered in the range $[0.001, 0.1]$ in Uriu et al. (2010), and $\nu_1^* \approx 0.25209$ obviously lies out of this interval.

Example 4.4 We compare the dynamics for the system modeled with linear degradations and the system modeled with Michaelis–Menten degradation. The Michaelis–Menten type degradation for the *her* mRNA is given by $f_1(x_1) = \nu_2 x_1/(k_2 + x_1)$ in

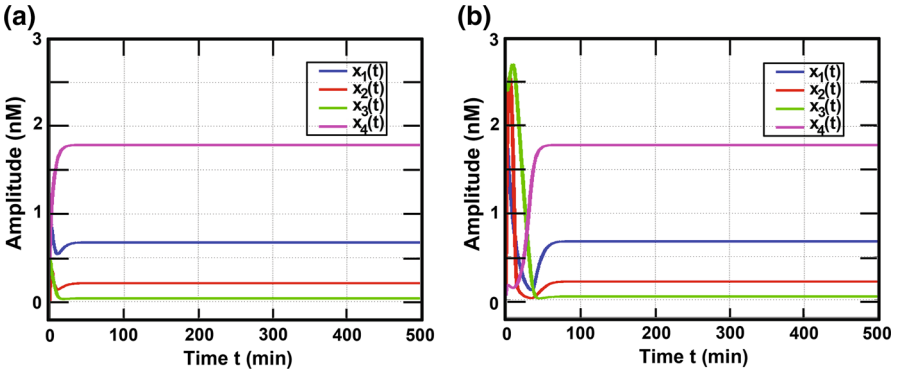

Fig. 4 The solutions (x_1, x_2, x_3, x_4) of system (37) with parameter values from Tables 1 and 2, evolved from initial value **a** $\phi = (1,\ 0.01,\ 0.5,\ 0.5)$, and **b** $\phi = (2,\ 0.1,\ 2.5,\ 0.05)$, appear to converge to constants

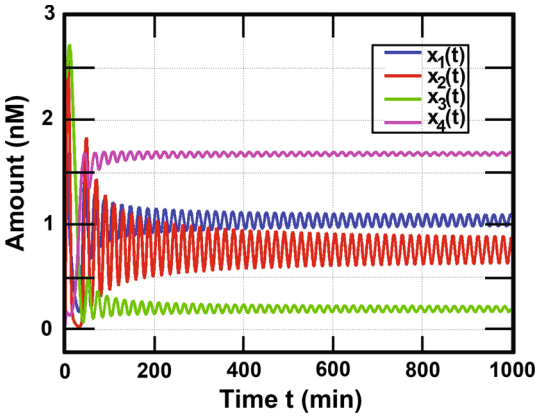

Fig. 5 The solution (x_1, x_2, x_3, x_4) of single-cell system (37) with parameter values in Tables 1 and 2, except that $\nu_1 = 0.069$ is replaced by $\nu_1 = 0.42$, evolved from initial value $\phi = (2, 0.1, 2.5, 0.05)$. The solution appears to converge to a periodic solution

(7). We take two linear functions with larger slope d_1^l and smaller slope d_1^s to approximate the graph of f_1 respectively. When $\nu_2 = 0.963, k_2 = 9.916$, the graph of f_1 is depicted in Fig. 6, where the graphs for linear functions with slopes $d_1^l = 0.095186$ and $d_1^s = 0.01067$ are also plotted. Similar approximations apply to f_2, f_3, f_4 with larger linear rates d_i^l and smaller linear rates $d_i^s, i = 2, 3, 4$, respectively. When $\nu_4 = 1.447, k_4 = 0.182, \nu_6 = 0.147, k_6 = 0.302, \nu_8 = 2.315, k_8 = 0.377$, we take $d_2^l = 4.892873, d_2^s = 0.188497, d_3^l = 0.274709, d_3^s = 0.026188, d_4^l = 3.835797, d_4^s = 0.460283$.

(i) We modify (8) by considering linear degradation in every component, i.e.,

$$\begin{cases} \dot{x}_1 = \dfrac{k_1^n}{k_1^n + x_3^n}(\nu_1 + \nu_c y_4) - d_1 x_1 \\ \dot{x}_2 = \nu_3 x_1 - d_2 x_2 - \nu_5 x_2 \\ \dot{x}_3 = \nu_5 x_2 - d_3 x_3 \\ \dot{x}_4 = \dfrac{\nu_7 k_7^h}{k_7^h + x_3^h} - d_4 x_4, \end{cases} \tag{38}$$

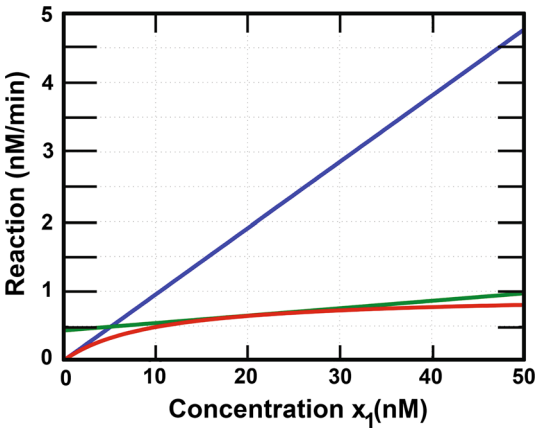

Fig. 6 The graph of Michaelis–Menten degradation for *her* mRNA, with $\nu_2 = 0.963$, $k_2 = 9.916$. The *blue line* is the linear degradation with larger rate $d_1^l = 0.095186$, and the *green line* is the linear degradation with smaller rate $d_1^s = 0.01067$ (color figure online)

for x-components, and similarly for the y-components. If we take $d_i = d_i^l, i = 1, 2, 3, 4$ or $d_i = d_i^s, i = 1, 2, 3, 4$, and the same values for the other parameters as in Example 4.1, numerical simulations indicate that all solutions converge to an equilibrium.

(ii) We employ linear degradations for x_1, x_4, y_1, y_4, while keeping Michaelis–Menten degradations for x_2, x_3, y_2, y_3, i.e.,

$$\begin{cases} \dot{x}_1 = \dfrac{k_1^n}{k_1^n + x_3^n}(\nu_1 + \nu_c y_4) - d_1 x_1 \\ \dot{x}_2 = \nu_3 x_1 - \dfrac{\nu_4 x_2}{k_4 + x_2} - \nu_5 x_2 \\ \dot{x}_3 = \nu_5 x_2 - \dfrac{\nu_6 x_3}{k_6 + x_3} \\ \dot{x}_4 = \dfrac{\nu_7 k_7^h}{k_7^h + x_3^h} - d_4 x_4, \end{cases} \tag{39}$$

for x-components, and similarly for the y-components. Let us use the linear degradation with larger slopes $d_1 = d_1^l$, $d_4 = d_4^l$ to approximate the Michaelis–Menten degradation, and take the same values for the other parameters (except ν_c) as in Example 4.1. Then synchronous periodic solutions emerge. Herein, ν_c can serve as a bifurcation parameter, and the Hopf bifurcation occurs at $\nu_c^* \approx 0.774146$. We fix $\nu_c = 0.78$ and vary only d_4, the periods and amplitudes for the periodic solutions are plotted in Fig. 7. It appears that the periods and amplitudes decrease as d_4 increases.

(iii) We use linear degradations with smaller rates $d_1 = d_1^s$ and $d_4 = d_4^s$ in (39) to approximate the Michaelis–Menten degradations. Choosing ν_c as the bifurcation parameter, it can be shown that Hopf bifurcation occurs at $\nu_c^* \approx 0.072545$. We fix $\nu_c = 0.074$ and vary only d_4. The periods and amplitudes of the periodic solutions appear to decrease as d_4 increases, as shown in Fig. 8.

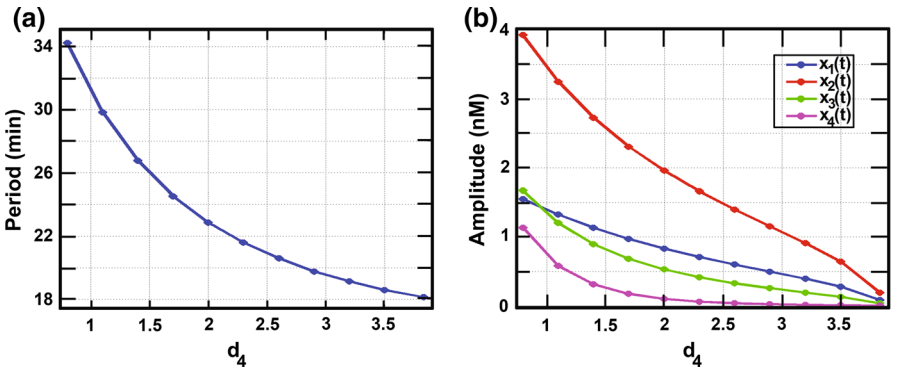

Fig. 7 The periods and amplitudes of the oscillations corresponding to various values of d_4 for system (39) with larger degradation rates

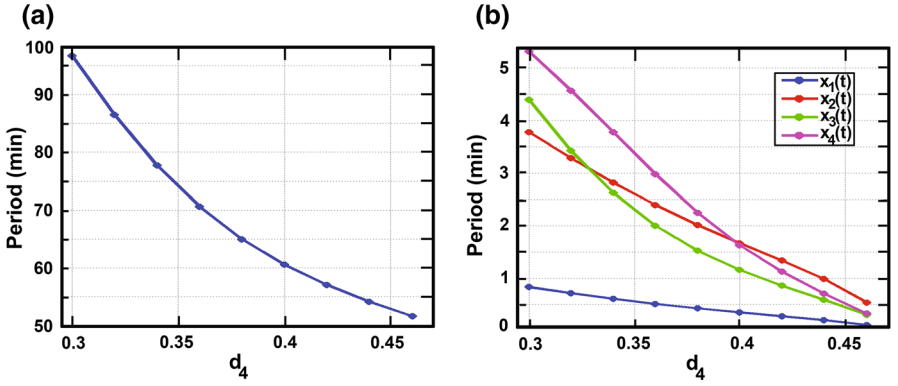

Fig. 8 The periods and amplitudes of the oscillations corresponding to various values of d_4 for system (39) with smaller degradation rates

4.2 Delay model (9)

In this subsection, we discuss stable synchronous periodic orbits in delay model (9) with $\tau_i > 0, i = 1, 2, 4$, via delay Hopf bifurcation theory. We shall consider that all parameters and τ_4 are fixed and take $r = \tau_1 + \tau_2$ as the bifurcation parameter. One can also take τ_4 as a bifurcation parameter.

Assume that the synchronous equilibrium $\bar{\mathbb{X}}$ of system (9) exists, as in Sect. 4.1. We consider system (17) which is a translation of (9) from the synchronous equilibrium $\bar{\mathbb{X}}$ to the origin. The linearization of system (17) at the origin is given by

$$\begin{cases} \dot{u}_1(t) = -d_1 u_1(t) - \gamma_1 u_3(t-\tau_1) + \gamma_2 v_4(t-\tau_1) \\ \dot{u}_2(t) = -d_2 u_2(t) + \nu_3 u_1(t-\tau_2) \\ \dot{u}_3(t) = -d_3 u_3(t) + \nu_5 u_2(t) \\ \dot{u}_4(t) = -d_4 u_4(t) - \gamma_3 u_3(t-\tau_4) \\ \dot{v}_1(t) = -d_1 v_1(t) - \gamma_1 v_3(t-\tau_1) + \gamma_2 u_4(t-\tau_1) \\ \dot{v}_2(t) = -d_2 v_2(t) + \nu_3 v_1(t-\tau_2) \\ \dot{v}_3(t) = -d_3 v_3(t) + \nu_5 v_2(t) \\ \dot{v}_4(t) = -d_4 v_4(t) - \gamma_3 v_3(t-\tau_4), \end{cases} \tag{40}$$

where $d_1,\ d_2,\ d_3,\ d_4,\ \gamma_1,\ \gamma_2$, and γ_3 are defined as (28) and (29), and are positive.

The characteristic equation for (40) is $\triangle(\lambda, \tau_1, \tau_2, \tau_4) = 0$, where $\triangle(\lambda, \tau_1, \tau_2, \tau_4)$ is given by

$$\det \begin{pmatrix} \lambda + d_1 & 0 & \gamma_1 e^{-\tau_1\lambda} & 0 & 0 & 0 & 0 & -\gamma_2 e^{-\tau_1\lambda} \\ -\nu_3 e^{-\tau_2\lambda} & \lambda + d_2 & 0 & 0 & 0 & 0 & 0 & 0 \\ 0 & -\nu_5 & \lambda + d_3 & 0 & 0 & 0 & 0 & 0 \\ 0 & 0 & \gamma_3 e^{-\tau_4\lambda} & \lambda + d_4 & 0 & 0 & 0 & 0 \\ 0 & 0 & 0 & -\gamma_2 e^{-\tau_1\lambda} & \lambda + d_1 & 0 & \gamma_1 e^{-\tau_1\lambda} & 0 \\ 0 & 0 & 0 & 0 & -\nu_3 e^{-\tau_2\lambda} & \lambda + d_2 & 0 & 0 \\ 0 & 0 & 0 & 0 & 0 & -\nu_5 & \lambda + d_1 & 0 \\ 0 & 0 & 0 & 0 & 0 & 0 & \gamma_3 e^{-\tau_4\lambda} & \lambda + d_4 \end{pmatrix}.$$

By letting $r := \tau_1 + \tau_2$, the characteristic equation can be factored as

$$\triangle_+(\lambda, \tau_1, \tau_2, \tau_4) \cdot \triangle_-(\lambda, \tau_1, \tau_2, \tau_4) = \triangle_+(\lambda, r, \tau_4) \cdot \triangle_-(\lambda, r, \tau_4) = 0, \tag{41}$$

where

$$\begin{aligned} \triangle_\pm(\lambda, r, \tau_4) := {} & \lambda^4 + \beta_1\lambda^3 + \beta_2\lambda^2 + \beta_3\lambda + \beta_4 \\ & + \nu_3\nu_5\gamma_1(\lambda + d_4)e^{-r\lambda} \pm \nu_3\nu_5\gamma_2\gamma_3 e^{-(r+\tau_4)\lambda}, \end{aligned} \tag{42}$$

and $\beta_i, i = 1, 2, 3, 4$, are given in (31). From the structure of the characteristic equation, we employ $r = \tau_1 + \tau_2$ as the bifurcation parameter, while holding τ_4 fixed. We will analyze the existence of periodic solutions bifurcating from the origin of (17) for r near the bifurcation value.

Assume that all parameters and τ_4 are fixed. We need to carry out the following steps to apply delay Hopf bifurcation theorem. Set $\sigma = +$ or $-$.

(I) Find a pair of purely imaginary characteristic values $\lambda_\sigma = \pm i\omega_\sigma$ with $\omega_\sigma > 0$ and the corresponding bifurcation values $\{r_\sigma^{(k)}(\omega_\sigma)\}_{k\in\mathbb{Z}}$ such that $\triangle_\sigma(\pm i\omega_\sigma, r_\sigma^{(k)}(\omega_\sigma), \tau_4) = 0$, for all $k \in \mathbb{Z}$.
(II) Examine that $i\omega_\sigma$ is a simple purely imaginary characteristic value.
(III) Examine the transversality: $\mathrm{Re}\lambda'(r_\sigma^{(k)}(\omega_\sigma)) \neq 0$, for some $k \in \mathbb{Z}$.

For step (I), we substitute $\lambda = i\omega$, into the characteristic equation (42), i.e., $\triangle_\pm(i\omega, r, \tau_4) = \tilde{R}_\pm(i\omega, r, \tau_4) + i\tilde{I}_\pm(i\omega, r, \tau_4) = 0$, where the real and imaginary parts are respectively

$$\begin{cases} \tilde{R}_\pm(i\omega, r, \tau_4) = \omega^4 - \beta_2\omega^2 + \beta_4 + \nu_3\nu_5\gamma_1\omega\sin(r\omega) + d_4\nu_3\nu_5\gamma_1\cos(r\omega) \\ \qquad\qquad \pm\nu_3\nu_5\gamma_2\gamma_3\cos((r+\tau_4)\omega) = 0 \\ \tilde{I}_\pm(i\omega, r, \tau_4) = -\beta_1\omega^3 + \beta_3\omega + \nu_3\nu_5\gamma_1\omega\cos(r\omega) - d_4\nu_3\nu_5\gamma_1\sin(r\omega) \\ \qquad\qquad \mp\nu_3\nu_5\gamma_2\gamma_3\sin((r+\tau_4)\omega) = 0. \end{cases} \tag{43}$$

Through a manipulation by some trigonometric function properties (shown in "Appendix 3"), finding solution ω to $\triangle_{\pm}(i\omega, r, \tau_4) = 0$ becomes equivalent to solving

$$Q_{\pm}(\omega) = \nu_3^2\nu_5^2(d_4^2\gamma_1^2 + \gamma_2^2\gamma_3^2) =: \Gamma, \tag{44}$$

where

$$\begin{aligned} Q_{\pm}(\omega) = {} & \omega^8 + (\beta_1^2 - 2\beta_2)\omega^6 + (\beta_2^2 - 2\beta_1\beta_3 + 2\beta_4)\omega^4 \\ & + (\beta_3^2 - 2\beta_2\beta_4 - \nu_3^2\nu_5^2\gamma_1^2)\omega^2 \pm 2\nu_3^2\nu_5^2\gamma_1\gamma_2\gamma_3 \sin(\tau_4\omega)\omega \\ & + \beta_4^2 \mp 2d_4\nu_3^2\nu_5^2\gamma_1\gamma_2\gamma_3 \cos(\tau_4\omega). \end{aligned}$$

By considering the graphs of $Q_{\pm}$, we can derive a condition for the existence of solution to (44):

Proposition 7 (i) *For any fixed $\tau_4 \geq 0$, there exists a positive solution to $Q_+(\omega) = \Gamma$ if $Q_+(0) < \Gamma$, i.e.,*

$$0 < \beta_4 = d_1d_2d_3d_4 < \nu_3\nu_5(d_4\gamma_1 + \gamma_2\gamma_3). \tag{45}$$

(ii) *For any fixed $\tau_4 \geq 0$, each of $Q_-(\omega) = \Gamma$ and $Q_+(\omega) = \Gamma$ has a positive solution if $Q_-(0) < \Gamma$, i.e.,*

$$0 < \beta_4 = d_1d_2d_3d_4 < \nu_3\nu_5|\gamma_2\gamma_3 - d_4\gamma_1|. \tag{46}$$

Proposition 7 provides some conditions for the existence of purely imaginary characteristic values $\pm i\omega_\sigma$. Notice that the inequalities in (45) and (46) actually express relations among parameters, rather than specifying the range for β_4. Because of the trigonometric functions in $\triangle_\sigma$, there is a sequence of values $r = r_\sigma^{(k)}$, $k \in \mathbb{Z}$ at which the characteristic values $\pm i\omega_\sigma$ exist. The process for executing (I)-(III) is sketched in "Appendix 3", and the details are similar to those in Liao et al. (2012). With these executions, we obtain the following delay-induced Hopf bifurcation.

Theorem 4 *Let all parameters and $\tau_4 \geq 0$ be fixed. Assume that there exists a pair of purely imaginary characteristic values $\pm i\omega_+$ (resp., $\pm i\omega_-$) satisfying conditions in (II) and (III) for a $r_+^{(k)}(\omega_+) > 0$ (resp., $r_-^{(k)}(\omega_-) > 0$) at some $k \in \mathbb{Z}$. Then Hopf bifurcation occurs at $r = r_+^{(k)}(\omega_+)$ (resp., $r = r_-^{(k)}(\omega_-)$), and a periodic orbit bifurcates from the zero solution of system (17). Moreover, the periodic orbit bifurcating at $r_+^{(k)}(\omega_+) > 0$ is synchronous, while the one bifurcating at $r_-^{(k)}(\omega_-) > 0$ is asynchronous.*

We have discussed periodic solutions generated by r-induced Hopf bifurcation, where the bifurcation values $\{r_\sigma^{(k)}\}_{k\in\mathbb{Z}}$ form a sequence. This is typical in delay-induced Hopf bifurcations. Next, we discuss stability of the bifurcating periodic solution at the first bifurcation value.

If there exists a purely imaginary characteristic value $i\omega_\sigma$ at its corresponding bifurcation values $\{r_\sigma^{(k)}(\omega_\sigma)\}_{k\in\mathbb{Z}}$ such that $\triangle_\sigma(i\omega_\sigma, r_\sigma^{(k)}(\omega_\sigma), \tau_4) = 0$, for all $k \in \mathbb{Z}$ and $\sigma = +$ or $-$, then we define the first bifurcation value, r_c of r as

$$r_c := \min\{r : r = r_+^{(k)}(\omega_+) > 0 \text{ and } r = r_-^{(k)}(\omega_-) > 0, \quad \text{for all } k \in \mathbb{Z}\}. \tag{47}$$

Moreover, we denote by $i\omega_c$ the purely imaginary characteristic root of $\triangle(i\omega_c, r_c, \tau_4) = 0$. In "Appendix 4", we show that the r_c and ω_c are well defined under some condition.

The stability of bifurcating periodic solution of system (17) induced by $r = \tau_1 + \tau_2$, can be analyzed through carrying out the following steps:

(IV) Confirm that Hopf bifurcation occurs at $r = r_c$ and $\lambda = i\omega_c$.
(V) Confirm the stability of the equilibrium for $r < r_c$.
(VI) Analyze the stability of bifurcating periodic orbit, by constructing local coordinates for the two-dimensional center manifold $\mathscr{M}_0$ at $r = r_c$, with the center manifold theorem and normal form method.

Locating all roots of $\triangle(\cdot,\cdot,\cdot) = 0$ is highly nontrivial. Steps (IV) and (V) ensure that the first stability switch of the origin (from stability to instability) occurs at $r = r_c$, for any $\tau_4 \geq 0$. It will be shown in "Appendix 4" that the origin of system (17) is asymptotically stable when delays are zero, by the Routh–Hurwitz criterion. Moreover, this stability continues to hold for $r < r_c$ and any $\tau_4 \geq 0$, under some conditions, as shown in Proposition 8 (in "Appendix 4"). The detail of step (VI) is arranged in "Appendix 5". In step (VI), there are certain terms g_{20}, g_{11}, g_{02}, and g_{21} derived from the vector field on $\mathscr{M}_0$. Subsequently, we obtain the following quantities which determine the direction and stability of the bifurcating periodic solution at the minimal bifurcation value r_c:

$$\begin{aligned}
C_1(r_c) &= \frac{i}{2\omega_c}\left(g_{20}g_{11} - 2|g_{11}|^2 - \frac{1}{3}|g_{02}|^2\right) + \frac{g_{21}}{2},\\
p_2 &= -\frac{\mathrm{Re}(C_1(r_c))}{\mathrm{Re}(\lambda'(r_c))},\\
\zeta_2 &= 2\mathrm{Re}(C_1(r_c)),\\
T_2 &= \frac{-1}{\omega_c}[\mathrm{Im}(C_1(r_c)) + p_2\mathrm{Im}(\lambda'(r_c))],
\end{aligned}$$

where $\lambda(r)$ is the eigenvalue crossing the imaginary axis at $r = r_c$, and $\lambda(r_c) = i\omega_c$. Computation of these terms and the following theorem can be found in Hassard et al. (1981).

Theorem 5 *Let all parameters and $\tau_4 \geq 0$ be fixed. Assume that system (17) undergoes a Hopf bifurcation at the origin at a minimal bifurcation value $r = r_c$, and the conditions in (V) hold.*

(i) *If $p_2 > 0$ (resp., < 0), then the bifurcation is supercritical (resp., subcritical) and a periodic solution bifurcates for $r > r_c$ (resp., $r < r_c$) with r near r_c.*

(ii) *If $\zeta_2 < 0$ (resp., > 0), then the bifurcating periodic solution is stable (resp., unstable).*

(iii) *If $T_2 > 0$ (resp., < 0) and $p_2 > 0$, then the period increases (resp., decreases) as r increases. If $T_2 < 0$ (resp., > 0) and $p_2 < 0$, then the period increases (resp., decreases) as r decreases.*

According to Theorems 4 and 5, let us summarize the criteria for the occurrence of stable synchronous and asynchronous oscillations, respectively.

Condition (S): The minimal bifurcation value r_c and the corresponding purely imaginary characteristic value $i\omega_c$ exist such that $\triangle_+(i\omega_c, r_c, \tau_4) = 0$; the equilibrium $\bar{\mathbb{X}}$ is asymptotically stable for $r < r_c$; the Hopf bifurcation occurs at r_c, and $\zeta_2 < 0$.

Condition (AS): The minimal bifurcation value r_c and the corresponding purely imaginary characteristic value $i\omega_c$ exist such that $\triangle_-(i\omega_c, r_c, \tau_4) = 0$; the equilibrium $\bar{\mathbb{X}}$ is asymptotically stable for $r < r_c$; the Hopf bifurcation occurs at r_c, and $\zeta_2 < 0$.

Corollary 1 *If condition (S) (resp., (AS)) holds for the parameters and τ_4 at some fixed values, then there exists a stable synchronous (resp., asynchronous) periodic solution of system (17), for $|r - r_c|$ small and $r > r_c$ if $p_2 > 0$, and $r < r_c$ if $p_2 < 0$.*

Remark 3 (i) For the delay model (9), while holding all parameters and τ_4 fixed, there could be a phase exchange between synchronous oscillation and asynchronous oscillation, as r varies. We shall illustrate this in the following subsection.

(ii) The conditions in Theorems 4 and 5 can all be examined numerically. In addition, the analysis in this subsection can be extended to coupled-cell system with four time delays, τ_1, τ_2, τ_3, and τ_4, where τ_3 is the time lag for the process of translocation.

4.2.1 Numerical illustrations

In this subsection, we perform several numerical simulations to illustrate the dynamical scenarios for system (9), and connect the dynamics to the somitogenesis mechanism. We first illustrate Theorem 4 by Example 4.5, then pursue extended numerical findings to explore further dynamical scenarios and properties for system (9). In numerical simulations on the delay equations (9), when the conditions in Theorem 4 or Theorem 5 are met, periodic solution emerges if we choose r to be a little larger or smaller than the bifurcation value r_c. Often the periodic solution persists if we further increase or decrease the bifurcation parameter r.

Example 4.5 We consider the following parameters

$$\begin{aligned} &k_1 = 9.10888,\ k_2 = 8.94996,\ k_4 = 0.945435,\\ &k_6 = 9.94208,\ k_7 = 0.484885,\ k_8 = 9.90454,\\ &\nu_1 = 0.075653,\ \nu_2 = 8.07477,\ \nu_3 = 46.8125,\\ &\nu_4 = 1.83792,\ \nu_5 = 0.554856,\\ &\nu_6 = 2.28749,\ \nu_7 = 6.40892,\ \nu_8 = 6.73278,\\ &\nu_c = 0.335551,\ n = h = 2. \end{aligned} \tag{48}$$

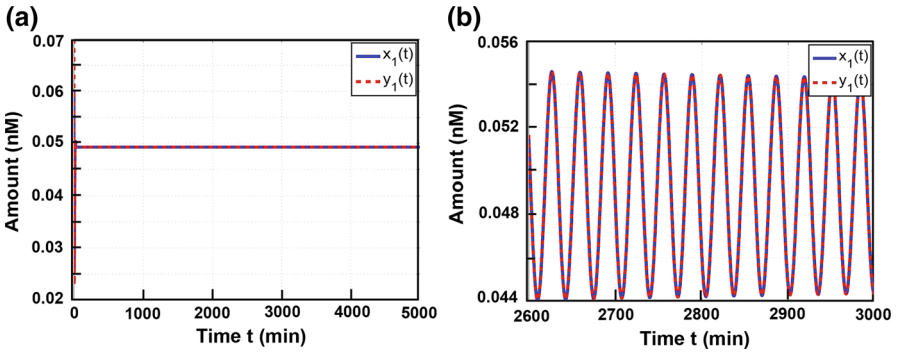

Fig. 9 The solution evolved from initial value $\phi = (0.06, 2.6, 17, 0.2, 0.07, 2.7, 18, 0.3)$, for **a** ODE system (8) with parameter values in (48), tends to the synchronous equilibrium $\bar{\mathbb{X}}$, **b** system (9) with delays in (49) and the same parameter values, tends to a stable synchronous solution

System (8) and system (9) both have a synchronous equilibrium at

$$\bar{\mathbb{X}} = (\bar{\mathbf{x}},\ \bar{\mathbf{x}}),\ \bar{\mathbf{x}} = (0.04928, 1.93335, 8.77964, 0.02875).$$

If there is no delay: $\tau_1 = \tau_2 = \tau_4 = 0$, i.e., considering system (8), then all eigenvalues of the linearized system at the equilibrium have negative real parts, as (33) is met. Thus, $\bar{\mathbb{X}}$ is asymptotically stable in system (8). Numerical simulation further indicates that all solutions converge to $\bar{\mathbb{X}}$ as $t \to \infty$, as demonstrated in Fig. 9a. It appears that there is no oscillation for ODE system (8) with parameters in (48).

On the other hand, if we consider delay system (9) with delays

$$\tau_1 = 3.86245,\ \tau_2 = 2.8,\ \tau_4 = 35, \tag{49}$$

then the solution evolved from the same initial value tends to a stable synchronous oscillation shown in Fig. 9b. The existence of this periodic solution follows from Theorem 4, by taking $\tau_1 + \tau_2$ to be near the minimal bifurcation value $\tau_c = 6.66245$. This example illustrates that when the ODE model (8) does not have oscillation, by adding suitable delays into the system, synchronous oscillation could be generated.

Example 4.6 Table 3 lists the ranges of all parameters considered in Uriu et al. (2010). We like to see how likely system (9) with delays is able to generate synchronous oscillation and asynchronous oscillation in these parameter ranges. We assume $\nu_8 > \nu_7$ so that the synchronous equilibrium exists, by Proposition 3. We take $\tau_2 = 2.8$, and respectively, $h = n = 1, 2, 3, 4$, $\tau_4 = 25, 35, 45, 55, 65, 75$, and then randomly choose 10,000 parameter sets of values from Table 3. We examine condition (S) and condition (AS) to determine the existence of stable synchronous and asynchronous periodic solutions when r near r_c, respectively. The numbers of parameter sets that satisfy each of these two conditions are recorded in Table 4.

In Table 4a, each denominator (resp., numerator) accounts for the number of parameter sets with which system (9) admits stable synchronous periodic solutions (resp.,

Table 3 The ranges of all parameters considered

	$k_1,\ k_2,\ k_4,\ k_6,\ k_7,\ k_8$	$\nu_2,\ \nu_4,\ \nu_6,\ \nu_7, \nu_8$	ν_1	ν_3	$\nu_5,\ \nu_c$
Range	0.1–10	0.1–10	0.001–0.1	0.5–50	0.01–1.0
Unit	nM	nM min^{-1}	nM min^{-1}	min^{-1}	min^{-1}

Table 4 For $\tau_4 = 25, 35, 45, 55, 65, 75$ and $n = h = 1, 2, 3, 4$, respectively, each denominator (resp., numerator) in (a) is the total number of parameter sets with which the system has a stable synchronous oscillation (resp., stable synchronous oscillation with period within [25, 35] min), when r is near r_c; (b) the total number of parameter sets with which the system has a stable asynchronous oscillation when r is near r_c

	$\tau_4 = 25$	$\tau_4 = 35$	$\tau_4 = 45$	$\tau_4 = 55$	$\tau_4 = 65$	$\tau_4 = 75$
(a) Synchronous oscillation						
$n = h = 1$	62/1141	196/1096	7/1006	140/992	107/936	63/929
$n = h = 2$	30/549	97/536	0/481	54/489	66/492	28/461
$n = h = 3$	20/332	60/312	1/296	43/321	37/291	19/277
$n = h = 4$	11/235	43/220	2/210	27/206	31/199	19/204
(b) Asynchronous oscillation						
$n = h = 1$	629	664	755	769	829	839
$n = h = 2$	366	382	438	426	424	456
$n = h = 3$	249	274	288	265	297	312
$n = h = 4$	201	216	224	228	239	233

stable synchronous periodic solutions with period within [25, 35] min), when r is near the minimal bifurcation value r_c (i.e., τ_1 near $r_c - \tau_2 = r_c - 2.8$). It appears in Table 4a that the most stable synchronous oscillations with period within [25, 35] min generated is when $n = h = 1$ and $\tau_4 = 35$. We also record in Table 4b the number of cases which generate stable asynchronous periodic solution, when r is near r_c.

We then perform a statistics to the data in Table 4 and collect the parameter values with which system (9) satisfies condition (S) and hence generates synchronous oscillation. As an illustration, we display the frequency histograms for the case $\tau_4 = 35$ and $n = h = 1$. Figure 10 indicates that parameters ν_6, ν_8, k_6 with $\nu_6 < 4$, $\nu_8 > 5$, and $k_6 > 5$ together tend to satisfy condition (S). Figure 11 indicates that $\nu_3 > 25$ or $\nu_4 < 5$ or $\nu_5 > 0.5$, or $\nu_7 < 5$ tends to satisfy condition (S). Hence, if the degradation rate ν_6 of Her protein in nucleus is small, and the degradation rate ν_8 of Delta protein is large, then the system tends to generate stable periodic solutions. In addition, we found that system with different Hill coefficients and τ_4 has similar distribution for synchronous and asynchronous oscillation. That is, the Hill coefficients do not affect significantly the parameter distribution for oscillation, and this is consistent with the observation in Uriu et al. (2010) for the ODE system (8).

Example 4.7 From our numerical simulations on system (9) with parameters satisfying condition (S) or condition (AS), we further observe the following properties:

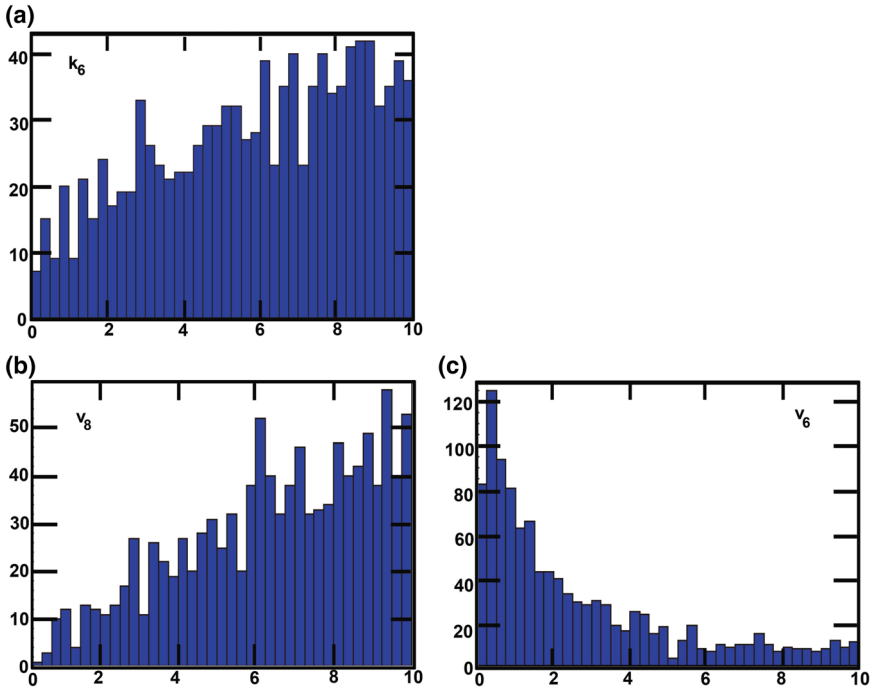

Fig. 10 The frequency histograms of the parameters k_6, ν_8, and ν_6 that the corresponding system generates stable synchronous oscillations when r near r_c, $\tau_4 = 35$, and $n = h = 1$

(i) Phase exchange: We choose two sets of parameter values from the computation in Table 4 to demonstrate the phase exchange between synchronous and asynchronous oscillations as bifurcation parameter r varies:

$$\begin{aligned}(k_1, k_2, k_4, k_6, k_7, k_8) &= (1.65443, 1.39621, 8.06972, 8.61674,\\ &\quad 9.71803, 3.87536),\\ (\nu_1, \nu_2, \nu_3, \nu_4, \nu_5, \nu_6, \nu_7, \nu_8, \nu_c) &= (0.075602, 2.07115, 10.9502, 5.59773,\\ &\quad 0.1928248, 2.02374, 5.26644, 7.09196,\\ &\quad 0.591048), \qquad (50)\\ (k_1, k_2, k_4, k_6, k_7, k_8) &= (0.847943, 1.4226, 4.90274, 1.35171,\\ &\quad 5.89576, 3.91132),\\ (\nu_1, \nu_2, \nu_3, \nu_4, \nu_5, \nu_6, \nu_7, \nu_8, \nu_c) &= (0.011547, 3.30484, 30.2745, 0.835863,\\ &\quad 0.685058, 1.34702, 0.362676, 5.74838,\\ &\quad 0.587321). \qquad (51)\end{aligned}$$

System (9) with parameters (50) (resp., (51)) satisfies condition (S) (resp., (AS)) with minimal bifurcation value r_c^s (resp., r_c^a). When r is near r_c^s (resp., r_c^a), there exists a stable synchronous (resp., asynchronous) periodic solution bifur-

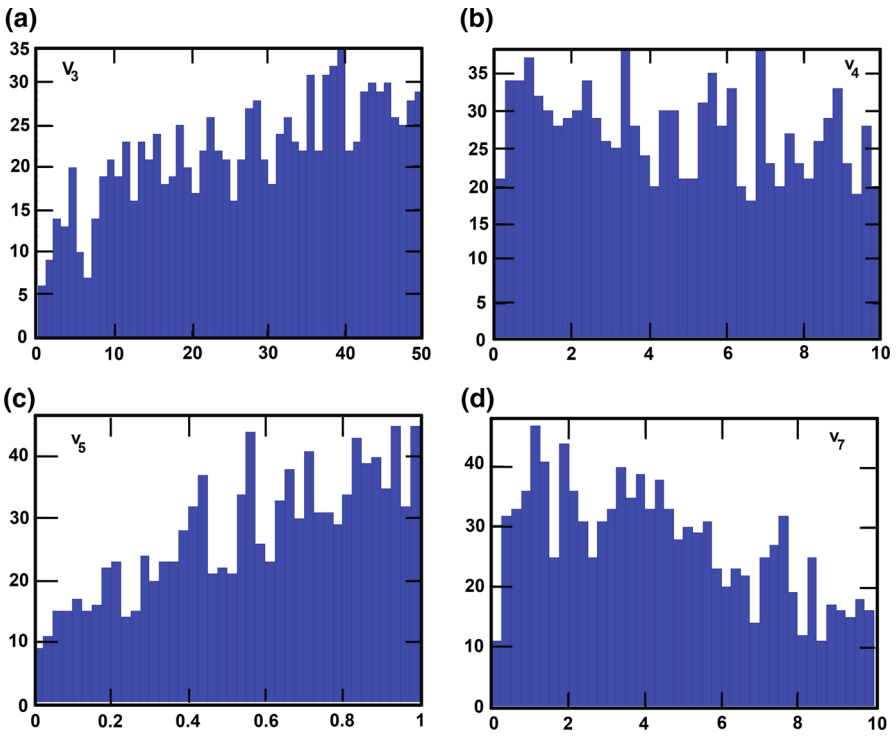

Fig. 11 The frequency histograms of the parameters ν_3, ν_4, ν_5, and ν_7 that the corresponding system generates stable synchronous oscillations when r near r_c, $\tau_4 = 35$, and $n = h = 1$

cating from the equilibrium $\bar{\mathbb{X}}$, by Corollary 1. If we take r near r_c^s (resp., r_c^a), and then increase it to another bifurcation value larger than r_c^s (resp., r_c^a), then the system undergoes a phase exchange from synchronous (resp., asynchronous) oscillation to asynchronous (resp., synchronous) oscillation, as shown in Fig. 12 (resp., Fig. 13). In addition, if we set delays to zeros, then these periodic solutions disappear, as shown in Fig. 14. Restated, holding a suitable τ_4 and varying r could generate a sequence of phase exchanges between synchronous and asynchronous oscillations, and the oscillation disappears when delays are all zeros. In Figs. 12, 13 and 14, we plot components $x_1(t)$ and $y_1(t)$ of the solution evolved from the initial value $\phi = (0.1, 0.1, 0.1, 0.1, 0.2, 0.2, 0.2, 0.2)$.

(ii) Existence of stable synchronous or asynchronous periodic solution depends sensitively on the magnitudes of delays r and τ_4. One may not be able to find a periodic solution when the value of r is not close enough to a bifurcation value.

(iii) We observe that the system tends to generate stable synchronous oscillations with a period about 30 min, if the system satisfies condition (S) and $r_c < 10$.

(iv) For a set of fixed parameter values, the period of bifurcating periodic solution is larger at larger bifurcation value. On the other hand, for system (9) with parameters which yield larger minimal bifurcation value, the periodic solution bifurcating at such value has larger period.

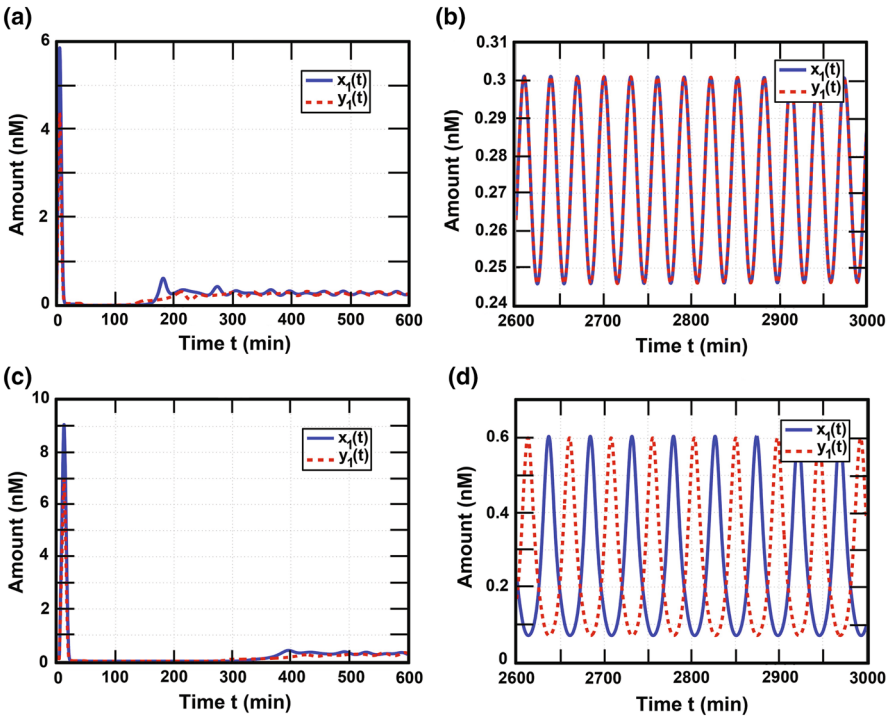

Fig. 12 With $\tau_4 = 35$, the parameter values in (50), and $r = 3.401106$ near r_c^s, in **a** $t \in [0, 600]$, **b** $t \in [2600, 3000]$, and $r = 6.04389$ near certain bifurcation value larger than r_c^s in **c** $t \in [0, 600]$, **d** $t \in [2600, 3000]$, the system undergoes a phase exchange from a stable synchronous oscillation to a stable asynchronous oscillation

5 Comparison between models

In this section, we summarize the dynamical properties according to our theories in Sects. 3 and 4 and subsequent numerical computations, and make a comparison between ODE model (8) and delay model (9). Such a comparison and the study on whether the ODE model (8) or delay model (9) is more suitable for modeling the segmentation clock have been an appealing research interest, as mentioned in the Introduction.

Let us classify the basic dynamics for (9) with respect to parameters. Recall $\beta_4 = d_1d_2d_3d_4$ defined in (31) and $\check{\beta}_4 := \check{d}_1\check{d}_2\check{d}_3\check{d}_4$ defined in (20). We introduce intervals

$$I_1 := (0, \nu_3\nu_5|\gamma_2\gamma_3 - d_4\gamma_1|),$$
$$I_2 := (\nu_3\nu_5|\gamma_2\gamma_3 - d_4\gamma_1|, \nu_3\nu_5(\gamma_2\gamma_3 + d_4\gamma_1)),$$

shown in Fig. 15a. According to Proposition 8 (in "Appendix 4"), and (25) in Remark 2(i), we summarize:

(i) If $\beta_4 < \nu_3\nu_5|\gamma_2\gamma_3 - d_4\gamma_1|$, i.e., $\beta_4 \in I_1$, then there exist $i\omega_+, i\omega_-, \{r_+^{(k)}(\omega_+)\}_{k\in\mathbb{Z}}$, $\{r_-^{(k)}(\omega_-)\}_{k\in\mathbb{Z}}$ such that $\triangle_+(i\omega_+, r_+^{(k)}(\omega_+), \tau_4) = 0$ and $\triangle_-(i\omega_-, r_-^{(k)}(\omega_-), \tau_4) = 0$, for all $k \in \mathbb{Z}$.

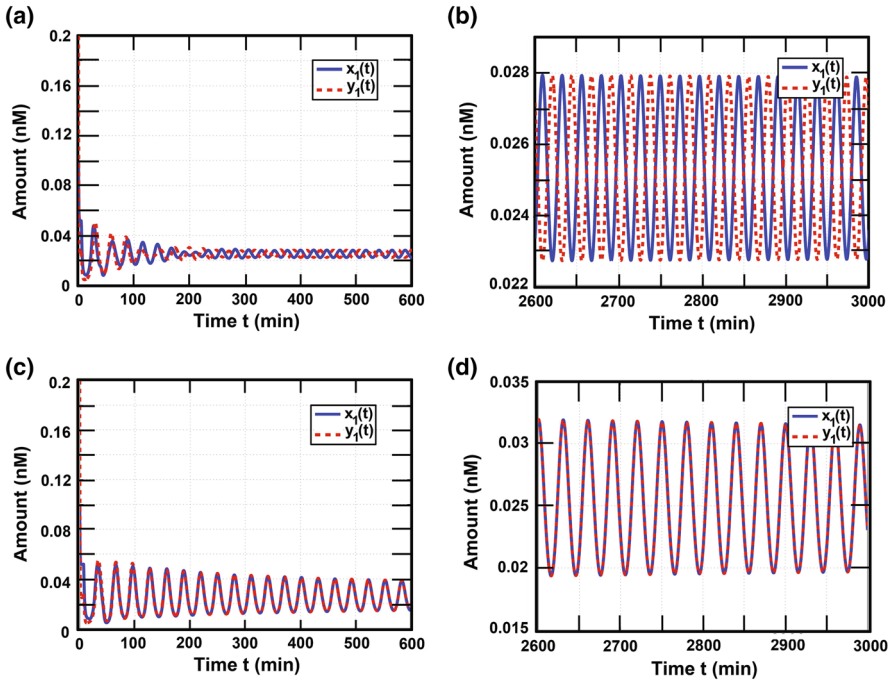

Fig. 13 With $\tau_4 = 35$, the parameter values in (51), and $r = 7.15282$ near r_c^a in **a** $t \in [0, 600]$, **b** $t \in [2600, 3000]$, and $r = 9.14428$ near certain bifurcation value larger than r_c^a in **c** $t \in [0, 600]$, **d** $t \in [2600, 3000]$, the system undergoes a phase exchange from a stable asynchronous oscillation to a stable synchronous oscillation

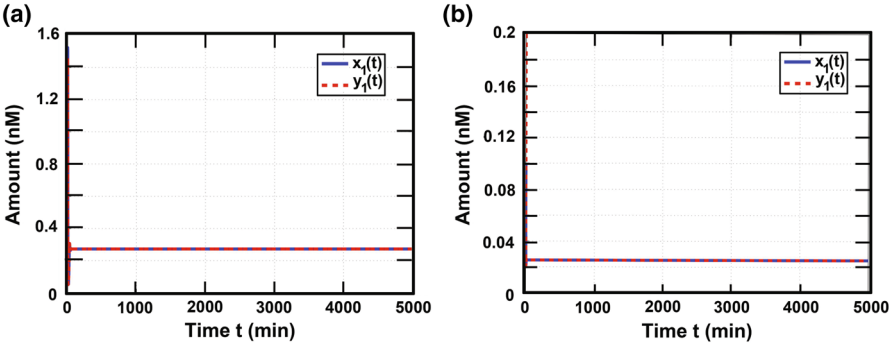

Fig. 14 With $r = \tau_4 = 0$, and the parameter values in **a** (50) and **b** (51), the solution tends to an equilibrium

(ii) If $\nu_3\nu_5|\gamma_2\gamma_3 - d_4\gamma_1| < \beta_4 < \nu_3\nu_5(\gamma_2\gamma_3 + d_4\gamma_1)$, i.e., $\beta_4 \in I_2$, then there exist $i\omega_+$ and $\{r_+^{(k)}(\omega_+)\}_{k\in\mathbb{Z}}$ such that $\triangle_+(i\omega_+, r_+^{(k)}(\omega_+), \tau_4) = 0$, for all $k \in \mathbb{Z}$.

(iii) If $\check{\beta}_4 > \nu_3\nu_5(\hat{\rho}_1\check{d}_4 + \hat{\rho}_2\hat{\rho}_3)$, then there does not exist oscillation for both ODE system (8) and delay system (9).

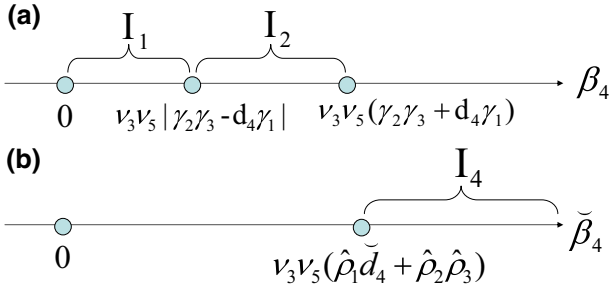

Fig. 15 **a** Partition for the range of β_4: $I_1 = (0, \nu_3\nu_5|\gamma_2\gamma_3 - d_4\gamma_1|)$, $I_2 = (\nu_3\nu_5|\gamma_2\gamma_3 - d_4\gamma_1|, \nu_3\nu_5(\gamma_2\gamma_3 + d_4\gamma_1))$. **b** Partition for the range of $\breve{\beta}_4$: $I_4 = (\nu_3\nu_5(\hat{\rho}_1\breve{d}_4 + \hat{\rho}_2\hat{\rho}_3), \infty)$. $\hat{\rho}_i$ is defined in (24), $i = 1, 2, 3$

Notably, $\breve{\beta}_4 \le \beta_4$, as $\breve{d}_i \le d_i$ for $i = 1, 2, 3, 4$, and $\gamma_i \le \hat{\rho}_i$, $i = 1, 2, 3$, where $\hat{\rho}_i$ is defined in (24). In addition, it has been shown in Lemma 2 that all eigenvalues of the linearized system of (8) at the equilibrium have negative real parts if and only if

$$\nu_3\nu_5(\gamma_2\gamma_3 - d_4\gamma_1) < \beta_4 < \frac{\alpha_1\alpha_2\alpha_3 - \alpha_3^2}{\alpha_1^2} - \nu_3\nu_5(d_4\gamma_1 + \gamma_2\gamma_3). \tag{52}$$

Therefore, if $\gamma_2\gamma_3 - d_4\gamma_1 > 0$, $\beta_4 \in I_2$, and β_4 lies in the range in (52), there does not exist synchronous periodic solution for the ODE system (8), through Hopf bifurcation. However, with such parameter values, synchronous periodic solution can exist for the delay system (9), according to delay Hopf bifurcation. In fact, Example 4.5 is such an instance. The Hopf bifurcation occurs for ODE system (8), when the right-hand inequality in (52) becomes equality, as seen in Proposition 6. Let us summarize the dynamical properties for systems (8) and (9):

- Synchronous oscillation: From our analytical and numerical results, it appears that the delay system (9) has wider parameter regime for synchronous periodic solution than the ODE system (8).
- Period with respect to coupling strength: In ODE system (8), the period of synchronous oscillation increases as the coupling strength increases, as shown in Fig. 3 in Example 4.2. This is in contrast to the finding in Herrgen et al. (2010), which was based on some experiment and the theory of coupled phase oscillator. On the other hand, it is possible that the period of synchronous oscillation increases as the coupling strength decreases in the delay system (9).
- Oscillation-arrested: For parameters satisfying (iii), both systems (8) and (9) admit global convergence to the synchronous equilibrium and there is no oscillation.
- Gradient structure: The gradient structure was adopted to generate traveling waves in N-cell systems extended from the cell–cell ODE system (8) in Uriu et al. (2009), and Lewis's delay system (2) in Liao and Shih (2012). Such wave patterns depict spatial-temporal oscillatory gene expression in the PSM of zebrafish. These oscillatory waves have larger periods at the anterior and smaller periods at the posterior of the PSM. For the delay system (9), construction of such traveling waves is also feasible. According to the analytical results in Sects. 3 and 4, the degradation

rates should be relatively large (resp., small) and the synthesis rates relatively small (resp., large) at the anterior (resp., posterior) of PSM to generate oscillation-arrested (resp., oscillation). We thus summarize the following distribution.

Distribution (D1): One of $k_1,\ k_2,\ k_4,\ k_6,\ k_7,\ k_8, \nu_1,\ \nu_3,\ \nu_c$ is relatively small (resp., large), or one of $\nu_2,\ \nu_4,\ \nu_6,\ \nu_8$ is relatively large (resp., small) to yield relatively large (resp., small) degradation rates and small (resp., large) synthesis rates for the cells located at the anterior (resp., posterior) of PSM.

In addition, from our numerical computation and Table 4, we see that relatively large (resp., small) ν_4 and ν_6 and relatively small (resp., large) k_6 and ν_3, which are consistent with the distribution (D1), tend to generate oscillation-arrested (resp., oscillation). On the other hand, the following distribution (D2) was adopted for the ODE system (8) to generate normal traveling wave pattern in Uriu et al. (2009).

Distribution (D2): One of $k_4,\ k_6,\ \nu_2,\ \nu_3,\ \nu_5,\ \nu_8$ is relatively small (resp., large), or one of $k_1,\ k_2,\ k_7,\ k_8,\ \nu_1,\ \nu_c$ is relatively large (resp., small) for the parameters corresponding to cells located at the anterior (resp., posterior) of PSM.

The distributions (D1) for delay system (9) and (D2) for ODE system (8) are disparate except $k_4,\ k_6$, and ν_3, and so the regimes for generating normal traveling wave patterns are distinct for these two systems.

6 Discussions and conclusions

In this paper, we analyzed the dynamics for two mathematical models on the kinetics of zebrafish segmentation clock genes. The ODE system (8) takes into account the translocation process in gene regulation to replace the consideration of time lags in transcription and translation. The delay system (9) includes these time delays into system (8). Mathematical analysis were performed to analyze the chief dynamics and locate the associated parameter regimes for both the delay and ODE systems. For oscillation-arrested, we derived conditions for global convergence to the synchronous equilibrium. For synchronous oscillations, we computed the characteristic equations of the linearized systems at the synchronous equilibrium for system (8) and system (9) respectively, and analyzed the characteristic values for each of these systems. With such computation, the Hopf bifurcation theory was applied to study the existence of synchronous periodic solutions for each of these systems, and asynchronous periodic solutions in delay system. For the ODE system, we took the synthesis rate of Delta protein or the activation rate of *her* mRNA transcription by Delta–Notch signal (coupling strength) as the bifurcation parameter. For the delay system, the sum of transcription delay and translation delay for *her* gene was used as the bifurcation parameter. Criterion for the existence of stable synchronous oscillations for each system was then established subsequently. Both systems admit the basic dynamical phases for segmentation clock genes and can accommodate the gradient structure associated with the traveling wave patterns.

It has been an interesting issue to investigate and distinguish what kind of mathematical models is more suitable to model gene regulation in somitogenesis. This is what we have pursued in this study. From our analysis and computation, it appears that the delay model (9) has wider parameter range for generating synchronous oscil-

lations. However, the synchrony of such oscillation depends on the magnitude of the delay tightly, and may yield to asynchronous oscillation at larger or smaller delay magnitudes. On the other hand, for the ODE system (8), we have seen that the period of the periodic solution increases with increasing coupling strength ν_c in Example 4.2. This is in contrast to the finding in the literature through experiments and the theory of coupled phase oscillators. In this regard, delay models appear to be more pertinent for modeling segmentation clock genes.

A mathematical reason for Lewis to consider delays in his model, (2) with (3), (4), is that, without adding delay, the dynamics for the decoupled single-cell system is determined by a two-dimensional ODE which can not generate oscillation, see Lewis (2003). On the other hand, for the decoupled single-cell system corresponding to (8), i.e., taking into account the translocation process and without adopting time delay, the dynamics is determined by a three-dimensional ODE, and thus can accommodate oscillations. However, the parameter values for such oscillation may not lie within the suitable range, as shown in Example 4.3.

Another issue is about the degradations. Mathematical models on segmentation clocks in the literature largely employ linear degradations. On the other hand, Michaelis–Menten type reactions for the degradation were adopted in Goldbeter and Pourquié (2008) and Uriu et al. (2009, 2010). From the view point of mathematical modeling, Michaelis–Menten reaction can be approximated by linear decay when the protein level is low (Murray 2002). However, some of the simulated protein levels in the literature are quite large (as large as hundreds). Certainly, the units for the variables and parameters will be important with this concern. We have illustrated in Example 4.4 that the dynamics in a system with linear degradations can be quite different from the ones in system with Michaelis–Menten degradations. Although some degradation rates were estimated from halflives of mRNA and proteins, experimental measurement of other reaction rates and quantifying some of the parameters will require further efforts, as mentioned in Ay et al. (2014) and Schwendinger-Schreck et al. (2014). These quantifications are also associated with what function forms the degradations are to be modeled with.

Systems (2), (8) and (9) actually represent typical forms of equations for modeling the kinetics of gene regulation in coupled cells. To investigate such somehow complicated equations, one certainly relies on numerical simulations. Nevertheless, assertions established from numerical simulations can certainly be strengthened by analytical supports. The analysis and techniques in this study are expected to provide a paradigm for mathematical investigation in other gene regulation models, in addition to the zebrafish somitogenesis.

Acknowledgements The authors are grateful to Chia-Chieh Jay Chu for his advice on computing the bifurcation value in ODEs. The authors were supported, in part, by the Ministry of Science and Technology, Taiwan.

Appendix 1: Proof of Theorem 2

Under the conditions of the theorem, the characteristic equation (30) has a pair of complex roots $R(\mu) \pm iI(\mu)$ for μ near μ^*. At $\mu = \mu^*$, this pair becomes purely

imaginary, and the other roots have negative real parts, i.e.,

$$R(\mu^*) = 0,\ I(\mu^*) > 0,$$

according to Proposition 6. Substituting $\lambda(\mu) = R(\mu) + iI(\mu)$ into Δ_+, and collecting the real and imaginary parts, we have

$$R^4 + \alpha_1 R^3 + \alpha_2 R^2 + \alpha_3 R + \alpha_4^+ - (6R^2 + 3\alpha_1 R + \alpha_2)I^2 + I^4 = 0, \quad (53)$$
$$I[-(4R + \alpha_1)I^2 + 4R^3 + 3\alpha_1 R^2 + 2\alpha_2 R + \alpha_3] = 0, \quad (54)$$

where $R = R(\mu)$, $I = I(\mu)$. If (54) has a solution with $I(\mu) \neq 0$, then

$$-(4R + \alpha_1)I^2 + 4R^3 + 3\alpha_1 R^2 + 2\alpha_2 R + \alpha_3 = 0.$$

Thus,

$$I^2 = \frac{4R^3 + 3\alpha_1 R^2 + 2\alpha_2 R + \alpha_3}{4R + \alpha_1}. \quad (55)$$

Substituting (55) into (53), using $\alpha_1(\mu^*)\alpha_2(\mu^*)\alpha_3(\mu^*) - \alpha_3^2(\mu^*) - \alpha_1^2(\mu^*)\alpha_4^+(\mu^*) = 0$, differentiating with respect to μ, and utilizing $R(\mu^*) = 0$ and $I(\mu^*) \neq 0$, we obtain

$$\frac{dR}{d\mu}(\mu^*) = \frac{\frac{d}{d\mu}[\alpha_1(\mu)\alpha_2(\mu)\alpha_3(\mu) - \alpha_3^2(\mu) - \alpha_1^2(\mu)\alpha_4^+(\mu)]|_{\mu=\mu^*}}{-2\alpha_1(\mu^*)[\alpha_1(\mu^*)\alpha_3(\mu^*) + (\frac{2\alpha_3(\mu^*)}{\alpha_1(\mu^*)} - \alpha_2(\mu^*))^2]} \neq 0,$$

by the assumption of the theorem. Thus the transversality condition is met. We conclude that system (8) undergoes a Hopf bifurcation at $\bar{\mathbb{X}}$ and $\mu = \mu^*$. □

Appendix 2: Stability of bifurcating periodic solution, ODE case

We express system (26) into the form:

$$\dot{\mathbb{X}} = A(\mu)\mathbb{X} + \mathbf{f}(\mathbb{X}, \mu),$$

where $\mathbb{X} = (x_1, \ldots, x_4, y_1, \ldots, y_4)$, $A(\mu)$ is the linear part, and $\mathbf{f} = (f_1, \ldots, f_8)$ is the nonlinear term. At $\mu = \mu^*$, $A(\mu^*)$ has a pair of purely imaginary eigenvalues $\lambda(\mu^*) = \pm i\omega_0$. Let us make a transformation so that the linear part is in normal form. We consider the change of variables $\mathbb{X} = P\mathbb{Z}$, where

$$P = \left[\ \mathrm{Im}(\mathbf{u})\ \mathrm{Re}(\mathbf{u})\ \mathbf{v}_3 \cdots \mathbf{v}_8\ \right]_{8\times 8},$$

and $\mathbf{u} \in \mathbb{R}^8$ is the eigenvector of $A(\mu^*)$ corresponding to the eigenvalue $i\omega_0$ and $\mathbf{v}_3, \ldots, \mathbf{v}_8$ are the generalized eigenvectors for the remaining eigenvalues. Thus

$$P^{-1}A(\mu^*)P = \begin{bmatrix} 0 & -\omega_0 & \vdots \\ \omega_0 & 0 & \vdots \\ \cdots & \cdots & D \end{bmatrix}, \tag{56}$$

where D is an 6×6 matrix. Then the transformed system becomes

$$\dot{\mathbb{Z}} = P^{-1}A(\mu)P\mathbb{Z} + \mathbf{F}(\mathbb{Z}, \mu),$$

where $\mathbb{Z} = (z_1, \ldots, z_8)$ and $\mathbf{F}(\mathbb{Z}, \mu) = P^{-1}\mathbf{f}(P\mathbb{Z}, \mu)$ with $\mathbf{F} = (F_1, \ldots, F_8)$. At $\mu = \mu^*, \mathbb{Z} = \mathbf{0}$, we define

$$\begin{aligned}
g_{11} &= \frac{1}{4}\left[\left(\frac{\partial^2 F_1}{\partial z_1^2} + \frac{\partial^2 F_1}{\partial z_2^2}\right) + i\left(\frac{\partial^2 F_2}{\partial z_1^2} + \frac{\partial^2 F_2}{\partial z_2^2}\right)\right], \\
g_{02} &= \frac{1}{4}\left[\left(\frac{\partial^2 F_1}{\partial z_1^2} - \frac{\partial^2 F_1}{\partial z_2^2} - 2\frac{\partial^2 F_2}{\partial z_1 \partial z_2}\right) + i\left(\frac{\partial^2 F_2}{\partial z_1^2} - \frac{\partial^2 F_2}{\partial z_2^2} + 2\frac{\partial^2 F_1}{\partial z_1 \partial z_2}\right)\right], \\
g_{20} &= \frac{1}{4}\left[\left(\frac{\partial^2 F_1}{\partial z_1^2} - \frac{\partial^2 F_1}{\partial z_2^2} + 2\frac{\partial^2 F_2}{\partial z_1 \partial z_2}\right) + i\left(\frac{\partial^2 F_2}{\partial z_1^2} - \frac{\partial^2 F_2}{\partial z_2^2} - 2\frac{\partial^2 F_1}{\partial z_1 \partial z_2}\right)\right], \\
G_{21} &= \frac{1}{8}\left[\left(\frac{\partial^3 F_1}{\partial z_1^3} + \frac{\partial^3 F_1}{\partial z_1 \partial z_2^2} + \frac{\partial^3 F_2}{\partial z_1^2 \partial z_2} + \frac{\partial^3 F_2}{\partial z_2^3}\right)\right. \\
&\quad \left. + i\left(\frac{\partial^3 F_2}{\partial z_1^3} + \frac{\partial^3 F_2}{\partial z_1 \partial z_2^2} - \frac{\partial^3 F_1}{\partial z_1^2 \partial z_2} - \frac{\partial^3 F_1}{\partial z_2^3}\right)\right].
\end{aligned}$$

Next, for $k = 3, \ldots, 8$, we set

$$\begin{aligned}
h_{11}^{k-2} &= \frac{1}{4}\left(\frac{\partial^2 F_k}{\partial z_1^2} + \frac{\partial^2 F_k}{\partial z_2^2}\right), \\
h_{20}^{k-2} &= \frac{1}{4}\left[\left(\frac{\partial^2 F_k}{\partial z_1^2} - \frac{\partial^2 F_k}{\partial z_2^2}\right) - 2i\left(\frac{\partial^2 F_k}{\partial z_1 \partial z_2}\right)\right],
\end{aligned}$$

and let $w_{11}^{k-2}, w_{20}^{k-2} \in \mathbb{C}^6$ be the solutions of

$$Dw_{11}^{k-2} = -h_{11}^{k-2}, \quad (D - 2i\omega_0 I)w_{20}^{k-2} = -h_{20}^{k-2},$$

where D is defined in (56). For $k = 3, \ldots, 8$, let

$$G_{110}^{k-2} = \frac{1}{2}\left[\left(\frac{\partial^2 F_1}{\partial z_1 \partial z_k} + \frac{\partial^2 F_2}{\partial z_2 \partial z_k}\right) + i\left(\frac{\partial^2 F_2}{\partial z_1 \partial z_k} - \frac{\partial^2 F_1}{\partial z_2 \partial z_k}\right)\right],$$
$$G_{101}^{k-2} = \frac{1}{2}\left[\left(\frac{\partial^2 F_1}{\partial z_1 \partial z_k} - \frac{\partial^2 F_2}{\partial z_2 \partial z_k}\right) + i\left(\frac{\partial^2 F_2}{\partial z_1 \partial z_k} + \frac{\partial^2 F_1}{\partial z_2 \partial z_k}\right)\right].$$

Then we define

$$g_{21} = G_{21} + \sum_{k=1}^{6}(2G_{110}^k w_{11}^k + G_{101}^k w_{20}^k).$$

Appendix 3: Sketch of steps (I)–(III) in Sect. 4.2

Step (I): For any fixed $\tau_4 \geq 0$, we substitute $\lambda = i\omega$ with $\omega > 0$ into the characteristic equation (42), i.e., $\triangle_{\pm}(i\omega, r, \tau_4) = \tilde{R}_{\pm}(i\omega, r, \tau_4) + i\tilde{I}_{\pm}(i\omega, r, \tau_4) = 0$, where the real and imaginary parts are respectively

$$\begin{cases} \tilde{R}_{\pm}(i\omega, r, \tau_4) = \omega^4 - \beta_2\omega^2 + \beta_4 + \nu_3\nu_5\gamma_1 w \sin(r\omega) + d_4\nu_3\nu_5\gamma_1 \cos(r\omega) \\ \qquad\qquad \pm\nu_3\nu_5\gamma_2\gamma_3 \cos((r+\tau_4)\omega) = 0 \\ \tilde{I}_{\pm}(i\omega, r, \tau_4) = -\beta_1\omega^3 + \beta_3\omega + \nu_3\nu_5\gamma_1\omega\cos(r\omega) - d_4\nu_3\nu_5\gamma_1 \sin(r\omega) \\ \qquad\qquad \mp\nu_3\nu_5\gamma_2\gamma_3 \sin((r+\tau_4)\omega) = 0. \end{cases} \tag{57}$$

By the properties of trigonometric functions, (57) can be written as

$$\begin{cases} \sqrt{L_{\pm}(\omega)} \cdot \sin(\phi_{\pm} + r\omega) = -\omega^4 + \beta_2\omega^2 - \beta_4 \\ \sqrt{L_{\pm}(\omega)} \cdot \cos(\phi_{\pm} + r\omega) = \beta_1\omega^3 - \beta_3\omega, \end{cases} \tag{58}$$

where $L_{\pm}(\omega) := [\nu_3\nu_5(d_4\gamma_1 \pm \gamma_2\gamma_3\cos(\tau_4\omega))]^2 + [\nu_3\nu_5(\gamma_1\omega \mp \gamma_2\gamma_3\sin(\tau_4\omega))]^2 > 0$, if ω is a solution of (58), and $\phi_{\pm} \in [0, 2\pi)$ with

$$\sin(\phi_{\pm}) = \nu_3\nu_5[d_4\gamma_1 \pm \gamma_2\gamma_3\cos(\tau_4\omega)]/\sqrt{L_{\pm}(\omega)},$$
$$\cos(\phi_{\pm}) = \nu_3\nu_5[\gamma_1 w \mp \gamma_2\gamma_3\sin(\tau_4\omega)]/\sqrt{L_{\pm}(\omega)}.$$

In order to find solution ω to (58), we sum up the square of equations (58) and obtain

$$Q_{\pm}(\omega) = \nu_3^2\nu_5^2(d_4^2\gamma_1^2 + \gamma_2^2\gamma_3^2) =: \Gamma,$$

where

$$\begin{aligned} Q_{\pm}(\omega) = {} & \omega^8 + (\beta_1^2 - 2\beta_2)\omega^6 + (\beta_2^2 - 2\beta_1\beta_3 + 2\beta_4)\omega^4 \\ & + (\beta_3^2 - 2\beta_2\beta_4 - \nu_3^2\nu_5^2\gamma_1^2)\omega^2 \\ & \pm 2\nu_3^2\nu_5^2\gamma_1\gamma_2\gamma_3 \sin(\tau_4\omega)\omega + \beta_4^2 \mp 2d_4\nu_3^2\nu_5^2\gamma_1\gamma_2\gamma_3\cos(\tau_4\omega). \end{aligned}$$

Since $Q_{\pm}(0) = \beta_4^2 \mp 2d_4\nu_3^2\nu_5^2\gamma_1\gamma_2\gamma_3$ and both $Q_+(\omega)$ and $Q_-(\omega)$ are strictly increasing eventually and blow up as $\omega \to \infty$, we thus establish Proposition 7.

Proposition 7 guarantees the existence of the minimal bifurcation value r_c and its corresponding purely imaginary eigenvalue $i\omega_c$. In the sequel, we denote by ω_+ (resp., ω_-) a positive solution to $Q_+(\cdot) = \Gamma$ (resp., $Q_-(\cdot) = \Gamma$). By using (58), we have

$$\begin{aligned} &\tan(\phi_\pm + r\omega) = S(\omega)/C(\omega),\\ &S(\omega) := -\omega^4 + \beta_2\omega^2 - \beta_4,\\ &C(\omega) := \beta_1\omega^3 - \beta_3\omega. \end{aligned} \tag{59}$$

Let $\sigma = +$ or $-$. For each solution ω_σ to Q_σ, there exists a sequence $\{r_\sigma^{(k)}(\omega_\sigma)\}_{k\in\mathbb{Z}}$:

$$r_\sigma^{(k)}(\omega_\sigma) := \begin{cases} \frac{1}{\omega_\sigma}\left[\tan^{-1}\left(\frac{S(\omega_\sigma)}{C(\omega_\sigma)}\right) - \phi_\sigma + 2k\pi\right], & \text{if } C(\omega_\sigma) > 0\,,\\ \frac{1}{\omega_\sigma}\left[\tan^{-1}\left(\frac{S(\omega_\sigma)}{C(\omega_\sigma)}\right) - \phi_\sigma + (2k-1)\pi\right], & \text{if } C(\omega_\sigma) < 0\,,\\ \frac{1}{\omega_\sigma}\left[\frac{3\pi}{2} - \phi_\sigma + 2k\pi\right], & \text{if } C(\omega_\sigma) = 0,\ S(w_\sigma) < 0,\\ \frac{1}{\omega_\sigma}\left[\frac{\pi}{2} - \phi_\sigma + 2k\pi\right], & \text{if } C(\omega_\sigma) = 0,\ S(\omega_\sigma) > 0, \end{cases}$$

such that $\triangle_\sigma(i\omega_\sigma, r_\sigma^{(k)}(\omega_\sigma), \tau_4) = 0$. To simplify the notation, we denote $r_\sigma^{(k)} := r_\sigma^{(k)}(\omega_\sigma)$ as the bifurcation value. In particular, we shall take into account the case that $r_\sigma^{(k)} > 0$ in the following discussions. Accordingly, a positive solution ω_+ (resp., ω_-) of $Q_+(\cdot) = \Gamma$ (resp., $Q_-(\cdot) = \Gamma$) corresponds to a pair of purely imaginary roots $\pm i\omega_+$ (resp., $\pm i\omega_-$) of $\triangle_+(\cdot, r_+^{(k)}, \tau_4) = 0$ (resp., $\triangle_-(\cdot, r_-^{(k)}, \tau_4) = 0$). This completes the first step.

Step (II): Since every solution of (58) is also a solution to Q_+ or Q_-, if $Q_\sigma^{'}(\omega_\sigma) \neq 0$, and all other positive solutions to $Q_+(\cdot) = \Gamma$ and $Q_-(\cdot) = \Gamma$ are not integer multiples of ω_σ, then $i\omega_\sigma$ is a simple purely imaginary eigenvalue, with $\sigma = +$ or $-$.

Step (III): The following conditions guarantee the transversality property:

$$\begin{aligned} &[R_\sigma(\omega_\sigma, r_\sigma^{(k)})]^2 + [I_\sigma(\omega_\sigma, r_\sigma^{(k)})]^2 \neq 0,\ W_{1,\sigma}^2(\omega_\sigma, r_\sigma^{(k)}) + W_{2,\sigma}^2(\omega_\sigma, r_\sigma^{(k)}) \neq 0,\\ &Q_{1,\sigma}(\omega_\sigma, r_\sigma^{(k)})W_{1,\sigma}(\omega_\sigma, r_\sigma^{(k)}) + Q_{2,\sigma}(\omega_\sigma, r_\sigma^{(k)})W_{2,\sigma}(\omega_\sigma, r_\sigma^{(k)}) \neq 0, \end{aligned}$$

where

$$\begin{aligned} R_\pm(\omega, r) :=\ & -3\beta_1\omega^2 + \beta_3 + \nu_3\nu_5[(1 - d_4 r)\gamma_1\cos(r\omega)\\ & \mp\gamma_2\gamma_3(r + \tau_4)\cos((r + \tau_4)\omega) - \gamma_1 r\omega\sin(r\omega)],\\ I_\pm(\omega, r) :=\ & -4\omega^3 + 2\beta_2\omega - \nu_3\nu_5[\gamma_1 r\omega\cos(r\omega) + (1 - d_4 r)\gamma_1\sin(r\omega)\\ & \mp\gamma_2\gamma_3(r + \tau_4)\sin((r + \tau_4)\omega)],\\ Q_{1,\pm}(\omega, r) :=\ & \nu_3\nu_5\omega[-\gamma_1\omega\cos(r\omega) + d_4\gamma_1\sin(r\omega) \pm \gamma_2\gamma_3\sin((r + \tau_4)\omega)],\\ Q_{2,\pm}(\omega, r) :=\ & \nu_3\nu_5\omega[d_4\gamma_1\cos(r\omega) + \gamma_1\omega\sin(r\omega) \pm \gamma_2\gamma_3\cos((r + \tau_4)\omega)],\\ W_{1,\pm}(\omega, r) :=\ & -3\beta_1\omega^2 + \beta_3 + \nu_3\nu_5[(1 - d_4 r)\gamma_1\cos(r\omega)\\ & \mp\gamma_2\gamma_3(r + \tau_4)\cos((r + \tau_4)\omega) - \gamma_1 r\omega\sin(r\omega)], \end{aligned}$$

$$W_{2,\pm}(\omega, r) := -4\omega^3 + 2\beta_2\omega - \nu_3\nu_5[\gamma_1 r\omega\cos(r\omega) + (1 - d_4 r)\gamma_1 \sin(r\omega) \mp\gamma_2\gamma_3(r + \tau_4)\sin((r + \tau_4)\omega)].$$

Appendix 4: Sketch of steps (IV) and (V) in Sect. 4.2

Step (IV): Let us consider the characteristic equation (41) with $r = 0$:

$$\triangle_+(\lambda, 0, \tau_4) \cdot \triangle_-(\lambda, 0, \tau_4) = 0. \tag{60}$$

Our goal is to derive the condition for parameters under which all roots of (60) have negative real parts for all $\tau_4 \geq 0$. If so, then the stability switch will not occur for any $\tau_4 \geq 0$ and $r = 0$. Moreover, for any fixed $\tau_4 \geq 0$, there is also no stability switch when $r < r_c$. Combining these properties, we can then confirm the asymptotical stability of the origin for system (17) for any $\tau_4 \geq 0$ and $r < r_c$.

We have seen that all characteristic values of (60) have negative real parts when $\tau_4 = 0$, under condition (33) or (34). Therefore, it suffices to show that all characteristic values of (60) remain to have negative real parts for any $\tau_4 \geq 0$ and $r = 0$.

Proposition 8 *For any $\tau_4 \geq 0$, all characteristic values of (60) have negative real parts if*

$$E_1 > 0, E_3 > 0, E_5 > 0, \tag{61}$$
$$\beta_4 > \nu_3\nu_5(\gamma_2\gamma_3 - d_4\gamma_1), \tag{62}$$

where

$$\begin{aligned} E_1 &= 2[d_1^2 d_2^2(d_3^2 + d_4^2) + (d_1^2 + d_2^2)d_3^2 d_4^2 + 2(d_1 d_2 d_3 - (d_1 \\ &\quad + d_2 + d_3)d_4^2)\nu_3\nu_5\gamma_1 + \nu_3^2\nu_5^2\gamma_1^2], \\ E_3 &= 4[d_1^2(d_2^2 + d_3^2 + d_4^2) + d_2^2(d_3^2 + d_4^2) + d_3^2 d_4^2 \\ &\quad - 2(d_1 + d_2 + d_3)\nu_3\nu_5\gamma_1], \\ E_5 &= 6(d_1^2 + d_2^2 + d_3^2 + d_4^2). \end{aligned} \tag{63}$$

Proof We substitute $\lambda = i\nu$ with $\nu \geq 0$ into $\triangle_\pm(\lambda, 0, \tau_4) = 0$ and collect the real and imaginary parts to obtain

$$\begin{cases} \mp\nu_3\nu_5\gamma_2\gamma_3\cos(r\nu) &= \nu^4 - \beta_2\nu^2 + \beta_4 + d_4\nu_3\nu_5\gamma_1 \\ \pm\nu_3\nu_5\gamma_2\gamma_3\sin(r\nu) &= -\beta_1\nu^3 + \nu(\nu_3\nu_5\gamma_1 + \beta_3). \end{cases} \tag{64}$$

Next, we sum up the square of equations (64) to get

$$E(\nu) = (\nu_3\nu_5\gamma_2\gamma_3)^2, \tag{65}$$

where

$$E(\nu) := \nu^8 + (\beta_1^2 - 2\beta_2)\nu^6 + [2d_4\nu_3\nu_5\gamma_1 + \beta_2^2 - 2\beta_1(\nu_3\nu_5\gamma_1 + \beta_3) + 2\beta_4]\nu^4 + [\nu_3^2\nu_5^2\gamma_1^2 + \beta_3^2 + 2\nu_3\nu_5\gamma_1(-d_4\beta_2 + \beta_3) - 2\beta_2\beta_4]\nu^2 + (d_4\nu_3\nu_5\gamma_1 + \beta_4)^2.$$

Then $E'(\nu) = 8\nu^7 + E_5\nu^5 + E_3\nu^3 + E_1\nu$, where E_1, E_3, E_5 are defined in (63). Thus $E(\nu)$ is strictly increasing on $[0, \infty)$, under condition (61). Moreover, it is straightforward to verify that $E(0) = (d_4\nu_3\nu_5\gamma_1 + \beta_4)^2 > (\nu_3\nu_5\gamma_2\gamma_3)^2$ if (62) holds. Consequently, $E(\nu) > (\nu_3\nu_5\gamma_2\gamma_3)^2$, for all $\nu \geq 0$, and hence for all $\nu \in \mathbb{R}$, as E is an even function. Therefore, there does not exist any real solution to (65) under conditions (61) and (62). The assertion thus follows from continuity of characteristic values. This completes the proof.

Step (V): Setting $\sigma = +$ (resp., $\sigma = -$) if $Q_+(\omega_c) = \Gamma$ (resp., $Q_-(\omega_c) = \Gamma$), the following conditions ensure that the Hopf bifurcation occurs at $r = r_c$ and $\lambda = i\omega_c$:

Condition (B1): $Q_\sigma^{'}(\omega_c) \neq 0$, and all other positive solutions to $Q_+(\cdot) = \Gamma$ and $Q_-(\cdot) = \Gamma$ satisfy $\omega \neq m\omega_c$ for any integer m;
Condition (B2): $[R_\sigma(\omega_c, r_c)]^2 + [I_\sigma(\omega_c, r_c)]^2 \neq 0$, $W_{1,\sigma}^2(\omega_c, r_c) + W_{2,\sigma}^2(\omega_c, r_c) \neq 0$, and $Q_{1,\sigma}(\omega_c, r_c)W_{1,\sigma}(\omega_c, r_c) + Q_{2,\sigma}(\omega_c, r_c)W_{2,\sigma}(\omega_c, r_c) \neq 0$.

Appendix 5: Stability of bifurcating periodic solution, delay case

Step (VI): The stability of the bifurcating periodic solution is determined by the nonlinear terms of the equations. The condition for the stability can be expressed after the equations are put in a suitable form, under the theory of center manifold and normal form. Let us outline the main process for this step, following Hassard et al. (1981), see also Liao et al. (2012) and Yu and Cao (2006).

We write system (17) into the form:

$$\dot{\mathbb{X}}(t) = L_\mu \mathbb{X}_t + G_\mu(\mathbb{X}_t), \tag{66}$$

where $\mathbb{X}(t) = (x_1(t), \ldots, x_4(t), y_1(t), \ldots, y_4(t))^T$, $\mathbb{X}_t(\theta) = \mathbb{X}(t+\theta)$, $\theta \in [-\tau_M, 0]$, $L_\mu : \mathscr{C} \to \mathbb{R}^8$ is a linear operator, and $G_\mu : \mathscr{C} \to \mathbb{R}^8$ is a nonlinear operator, and the phase space $\mathscr{C} := \mathscr{C}([-\tau_M, 0], \mathbb{R}_+^8)$ is a Banach space under the supremum norm $\|\phi\| = \sup\{|\phi(\theta)| : -\tau_M \leq \theta \leq 0\}$. We label these operators by $\mu := r - r_c = \tau_1 + \tau_2 - r_c$, for a fixed minimal bifurcation value r_c. Herein, L_μ is defined by

$$L_\mu\phi = M_0\phi(0) + M_1\phi(-\tau_1) + M_2\phi(-\tau_2) + M_4\phi(-\tau_4),$$

where

$$(M_0)_{ij} = \begin{cases} -d_1, & \text{if } ij = 11, 55 \\ -d_2, & \text{if } ij = 22, 66 \\ -d_3, & \text{if } ij = 33, 77 \\ -d_4, & \text{if } ij = 44, 88 \\ \nu_5, & \text{if } ij = 32, \text{ and } ij = 76 \\ 0, & \text{otherwise,} \end{cases}$$

$$(M_1)_{ij} = \begin{cases} -\gamma_1, & \text{if } ij = 13, \text{ and } ij = 57 \\ \gamma_2, & \text{if } ij = 18, \text{ and } ij = 54 \\ 0, & \text{otherwise,} \end{cases}$$

$$(M_2)_{ij} = \begin{cases} \nu_3, & \text{if } ij = 21, \text{ and } ij = 65 \\ 0, & \text{otherwise,} \end{cases}$$

$$(M_4)_{ij} = \begin{cases} -\gamma_3, & \text{if } ij = 43 \text{ and } ij = 87 \\ 0, & \text{otherwise,} \end{cases}$$

as expressed in (40), with d_1, d_2, d_3, d_4 and $\gamma_1, \gamma_2, \gamma_3$ defined in (28) and (29), respectively. In fact, according to the Riesz representation theorem, by choosing

$$\eta(\theta, \mu) = M_0\delta(\theta) + M_1\delta(\theta + \tau_1) + M_2\delta(\theta + \tau_2) + M_4\delta(\theta + \tau_4),$$

we see that

$$L_\mu\phi = \int_{-\tau_M}^{0} d\eta(\theta, \mu)\phi(\theta),$$

where $\delta(\cdot)$ is the Dirac delta function. For operator $G_\mu : \mathscr{C} \to \mathbb{R}^8$, its eight components are

$$\begin{aligned}
&m_{11}\phi_3^2(-\tau_1) + m_{12}\phi_3(-\tau_1)\phi_8(-\tau_1) + m_{13}\phi_8^2(-\tau_1) + m_{14}\phi_3^3(-\tau_1) \\
&\quad + m_{15}\phi_3^2(-\tau_1)\phi_8(-\tau_1) + m_{16}\phi_3(-\tau_1)\phi_8^2(-\tau_1) \\
&\quad + m_{17}\phi_8^3(-\tau_1) + m_{18}\phi_1^2(0) + m_{19}\phi_1^3(0) + \text{h.o.t.}, \\
&m_{21}\phi_2^2(0) + m_{22}\phi_2^3(0) + \text{h.o.t.}, \\
&m_{31}\phi_3^2(0) + m_{32}\phi_3^3(0) + \text{h.o.t.}, \\
&m_{41}\phi_3^2(-\tau_4) + m_{42}\phi_3^3(-\tau_4) + m_{43}\phi_4^2(0) + m_{44}\phi_4^3(0) + \text{h.o.t.}, \\
&m_{11}\phi_7^2(-\tau_1) + m_{12}\phi_7(-\tau_1)\phi_4(-\tau_1) + m_{13}\phi_4^2(-\tau_1) \\
&\quad + m_{14}\phi_7^3(-\tau_1) + m_{15}\phi_7^2(-\tau_1)\phi_4(-\tau_1) \\
&\quad + m_{16}\phi_7(-\tau_1)\phi_4^2(-\tau_1) + m_{17}\phi_4^3(-\tau_1) + m_{18}\phi_5^2(0) + m_{19}\phi_5^3(0) + \text{h.o.t.}, \\
&m_{21}\phi_6^2(0) + m_{22}\phi_6^3(0) + \text{h.o.t.}, \\
&m_{31}\phi_7^2(0) + m_{32}\phi_7^3(0) + \text{h.o.t.}, \\
&m_{41}\phi_7^2(-\tau_4) + m_{42}\phi_7^3(-\tau_4) + m_{43}\phi_8^2(0) + m_{44}\phi_8^3(0) + \text{h.o.t.},
\end{aligned}$$

successively, where $\phi = (\phi_1, \ldots, \phi_8)$, and

$$\begin{aligned}
m_{11} &:= \frac{1}{2}\frac{\partial^2 g_H}{\partial u^2}(\bar{x}_3, \bar{x}_4), m_{12} := \frac{\partial^2 g_H}{\partial u \partial v}(\bar{x}_3, \bar{x}_4), \\
m_{13} &:= \frac{1}{2}\frac{\partial^2 g_H}{\partial v^2}(\bar{x}_3, \bar{x}_4), m_{14} := \frac{1}{6}\frac{\partial^3 g_H}{\partial u^3}(\bar{x}_3, \bar{x}_4), \\
m_{15} &:= \frac{1}{2}\frac{\partial^3 g_H}{\partial u^2 \partial v}(\bar{x}_3, \bar{x}_4), m_{16} := \frac{1}{2}\frac{\partial^3 g_H}{\partial u \partial v^2}(\bar{x}_3, \bar{x}_4),
\end{aligned}$$

$$
\begin{aligned}
&m_{17} := \frac{1}{6}\frac{\partial^3 g_H}{\partial v^3}(\bar{x}_3, \bar{x}_4), m_{18} := -\frac{1}{2}f_1''(\bar{x}_1),\\
&m_{19} := -\frac{1}{6}f_1'''(\bar{x}_1), m_{21} := -\frac{1}{2}f_2''(\bar{x}_2),\\
&m_{22} := -\frac{1}{6}f_2'''(\bar{x}_2), m_{31} := -\frac{1}{2}f_3''(\bar{x}_3),\\
&m_{32} := -\frac{1}{6}f_3'''(\bar{x}_3), m_{41} := \frac{1}{2}g_D''(\bar{x}_3),\\
&m_{42} := \frac{1}{6}g_D'''(\bar{x}_3), m_{43} := -\frac{1}{2}f_4''(\bar{x}_4),\\
&m_{44} := -\frac{1}{6}f_4'''(\bar{x}_4).
\end{aligned}
$$

To put (66) in a suitable form, we define two operators on $\mathscr{C}^1 := \mathscr{C}^1([-\tau_M, 0], \mathbb{R}^8)$:

$$
(A_\mu\phi)(\theta) = \begin{cases} d\phi(\theta)/d\theta, & \theta \in [-\tau_M,\ 0),\\ \int_{-\tau_M}^0 d\eta(\zeta,\mu)\phi(\zeta), & \theta = 0, \end{cases}
$$

$$
(R_\mu\phi)(\theta) = \begin{cases} 0, & \theta \in [-\tau_M,\ 0),\\ G_\mu(\phi), & \theta = 0. \end{cases}
$$

Then (66) can be recast into

$$
\dot{\mathbb{X}}_t = A_\mu \mathbb{X}_t + R_\mu \mathbb{X}_t. \tag{67}
$$

The adjoint operator A_μ^* of A_μ can be computed as

$$
(A_\mu^*\psi)(\theta^*) = \begin{cases} -d\psi(\theta^*)/d\theta^*, & \theta^* \in (0,\ \tau_M],\\ \int_{-\tau_M}^0 d\eta^T(\zeta,\mu)\psi(-\zeta), & \theta^* = 0, \end{cases}
$$

where $\psi \in \mathscr{C}^1([0, \tau_M], \mathbb{R}^8)$. In the following computation, for convenience, we allow functions to take values in $\mathbb{C}^8$. We use the bilinear form

$$
\langle \psi, \phi\rangle = \overline{\psi}^T(0)\phi(0) - \int_{\theta=-\tau_M}^0 \int_{\xi=0}^{\theta} \overline{\psi}^T(\xi-\theta)d\eta(\theta)\phi(\xi)d\xi,
$$

for $\phi \in \mathscr{C}([-\tau_M, 0], \mathbb{C}^8)$, $\psi \in \mathscr{C}([0, \tau_M], \mathbb{C}^8)$, to determine the coordinates of the center manifold near the origin of (66), where $\eta(\theta) := \eta(\theta, 0)$.

Next, denote by $q(\theta)$ the eigenvector of $A := A_0$, and $q^*(\theta^*)$ of $A^* := A_0^*$ corresponding to purely imaginary eigenvalues $i\omega_c$ and $-i\omega_c$, respectively, namely,

$$
Aq(\theta) = i\omega_c q(\theta), \text{ and } A^*q^*(\theta^*) = -i\omega_c q^*(\theta^*). \tag{68}
$$

We also impose the normalized condition $\langle q^*, q\rangle = 1$ and $\langle q^*, \bar{q}\rangle = 0$. To this end, we assume that

$$
q(\theta) = q(0)e^{i\omega_c\theta},\ q^*(\theta^*) = q^*(0)e^{i\omega_c\theta^*}, \tag{69}
$$

for $\theta \in [-\tau_M, 0), \theta^* \in (0, \tau_M]$, and $q(0) = (q_1, \ldots, q_8)^T$, $q^*(0) = \frac{1}{\rho}(q_1^*, \ldots, q_8^*)^T$, where ρ, q_i and $q_i^*, i = 1, \ldots, 8$, are to be determined. Substituting (69) into (68) and evaluating at $\theta = 0$, we obtain

$$
\begin{aligned}
&q_1 = 1,\ q_2 = \frac{\nu_3 U_2}{V_2},\ q_3 = \frac{\nu_3\nu_5 U_2}{V_2 V_3},\ q_4 = \frac{\nu_3\nu_5\gamma_3 U_2 U_4}{V_2 V_3 V_4},\\
&q_5 = \frac{\overline{U}_4 V_4(\nu_3\nu_5\gamma_1 + \overline{U}_1\overline{U}_2 V_1 V_2 V_3)}{-\nu_3\nu_5\gamma_2\gamma_3},\ q_6 = \frac{\overline{U}_4 V_3 V_4(\overline{U}_1 V_1 V_2 V_3 + \nu_3\nu_5\gamma_1 U_2)}{-\nu_5\gamma_2\gamma_3 V_2 V_3},\\
&q_7 = \frac{\overline{U}_4 V_4(\overline{U}_1 V_1 V_2 V_3 + \nu_3\nu_5\gamma_1 U_2)}{-\gamma_2\gamma_3 V_2 V_3},\ q_8 = \frac{\overline{U}_1 V_1 V_2 V_3 + \nu_3\nu_5\gamma_1 U_2}{\gamma_2 V_2 V_3},\\
&q_1^* = 1,\ q_2^* = \frac{U_2\overline{V}_1}{\nu_3},\ q_3^* = \frac{U_2\overline{V}_1\overline{V}_2}{\nu_3\nu_5},\\
&q_4^* = \frac{\nu_3\nu_5\gamma_1\overline{U}_1 U_4 + U_2 U_4\overline{V}_1\overline{V}_2\overline{V}_3}{-\nu_3\nu_5\gamma_3},\ q_5^* = \frac{\nu_3\nu_5\gamma_1 U_4\overline{V}_4 + U_1 U_2 U_4\overline{V}_1\overline{V}_2\overline{V}_3\overline{V}_4}{-\nu_3\nu_5\gamma_2\gamma_3},\\
&q_6^* = -\frac{U_1 U_2^2 U_4\overline{V}_4(-\nu_3\nu_5\gamma_1\overline{U}_1\overline{U}_2\overline{V}_1 - \overline{V}_1^2\overline{V}_2\overline{V}_3)}{-\nu_3^2\nu_5\gamma_2\gamma_3},\\
&q_7^* = \frac{U_1 U_2^2 U_4\overline{V}_1\overline{V}_2\overline{V}_4(\nu_3\nu_5\gamma_1\overline{U}_1\overline{U}_2 + \overline{V}_1\overline{V}_2\overline{V}_3)}{-\nu_3^2\nu_5^2\gamma_2\gamma_3},\ q_8^* = \frac{\gamma_2\overline{U}_1}{\overline{V}_4},
\end{aligned}
$$

where $U_j = e^{-i\omega_c\tau_j}$, $j = 1, 2, 4$, and $V_j = i\omega_c + d_j$, for $j = 1, \ldots, 4$. Notice that $\langle q^*, q\rangle = 1$ and $\langle q^*, \bar{q}\rangle = 0$, if we set

$$
\begin{aligned}
\bar{\rho} = &(q_1\overline{q_1^*} + q_2\overline{q_2^*} + \cdots + q_8\overline{q_8^*})\\
&+ J_1\tau_1 e^{-i\omega_c\tau_1} + J_2\tau_2 e^{-i\omega_c\tau_2} + J_4\tau_4 e^{-i\omega_c\tau_4},
\end{aligned}
$$

where $J_1 := -\gamma_1(q_3\overline{q}_1^* + q_7\overline{q}_5^*) + \gamma_2(q_8\overline{q}_1^* + q_4\overline{q}_5^*)$, $J_2 := \nu_3(q_1\overline{q}_2^* + q_5\overline{q}_6^*)$, and $J_4 := -\gamma_3(q_3\overline{q}_4^* + q_7\overline{q}_8^*)$.

Now, we use q and q^* to construct a coordinate on the center manifold $\mathscr{M}_0$ at $\mu = 0$. For each $\phi \in \mathscr{C}([-\tau_M, 0], \mathbb{C}^8)$, we associate a pair (z, w), with $z = \langle q^*, \phi\rangle$, $w = \phi - zq - \overline{z}\overline{q} = \phi - 2\mathrm{Re}(zq)$. Let $\mathbb{X}_t = \mathbb{X}_t(\theta) = (x_{1,t}(\theta), \ldots, x_{4,t}(\theta), y_{1,t}(\theta), \ldots, y_{4,t}(\theta))^T$ be a solution of (67), and let

$$
\begin{aligned}
z(t) &:= \langle q^*,\ \mathbb{X}_t\rangle,\\
W(t, \theta) &:= \mathbb{X}_t(\theta) - 2\mathrm{Re}(z(t)q(\theta)).
\end{aligned}
$$

On the center manifold $\mathscr{M}_0$, $W(t, \theta) = w(z(t), \bar{z}(t), \theta)$, where

$$
w(z(t), \bar{z}(t), \theta) = w_{20}(\theta)\frac{z^2(t)}{2} + w_{11}(\theta)z(t)\bar{z}(t) + w_{02}(\theta)\frac{\bar{z}^2(t)}{2} + \cdots.
$$

Herein, z and $\bar{z}$ are the local coordinates of the center manifold $\mathscr{M}_0$ in directions q^* and $\overline{q^*}$, respectively.

Hence, the solution $\mathbb{X}_t \in \mathscr{M}_0$ of (67), at $\mu = 0$, satisfies

$$\dot{z}(t) = i\omega_c z(t) + g(z(t), \bar{z}(t)),$$

where

$$g(z,\bar{z}) = \overline{q^*}^T(0)G_0(z,\bar{z}) = g_{20}\frac{z^2}{2} + g_{11}z\bar{z} + g_{02}\frac{\bar{z}^2}{2} + g_{21}\frac{z^2\bar{z}}{2} + \cdots,$$

and

$$\begin{aligned}
g_{20} = \frac{2}{\bar{\rho}}\{&m_{18}(q_1^2\overline{q}_1^* + q_5^2\overline{q}_5^*) + m_{12}(q_2^2\overline{q}_2^* + q_6^2\overline{q}_6^*)\\
&+ m_{31}(q_3^2\overline{q}_3^* + q_7^2\overline{q}_7^*) + m_{43}(q_4^2\overline{q}_4^* + q_8^2\overline{q}_8^*)\\
&+ e^{-2i\omega_c\tau_1}[(m_{11}q_3^2 + q_8(m_{12}q_3 + m_{13}q_8))\overline{q}_1^* + (m_{13}q_4^2\\
&+ q_7(m_{12}q_4 + m_{11}q_7))\overline{q}_5^*] + e^{-2i\omega_c\tau_4}m_{41}(q_3^2\overline{q}_4^* + q_7^2\overline{q}_8^*)\},\\
g_{11} = \frac{1}{\bar{\rho}}\{&[2m_{18}q_1\overline{q}_1 + 2m_{11}q_3\overline{q}_3 + m_{12}(q_8\overline{q}_3 + q_3\overline{q}_8)\\
&+ 2m_{13}q_8\overline{q}_8]\overline{q}_1^* + (2m_{14}q_3\overline{q}_3 + 2m_{43}q_4\overline{q}_4)\overline{q}_4^*\\
&+ [2m_{13}q_4\overline{q}_4 + 2m_{18}q_5\overline{q}_5 + m_{12}(q_7\overline{q}_4 + q_4\overline{q}_7) + 2m_{11}q_7\overline{q}_7]\overline{q}_5^*\\
&+ (2m_{14}q_7\overline{q}_7 + 2m_{43}q_8\overline{q}_8)\overline{q}_8^* + 2m_{21}(q_2\overline{q}_2\overline{q}_2^* + q_6\overline{q}_6\overline{q}_6^*)\\
&+ 2m_{31}(q_3\overline{q}_3\overline{q}_3^* + q_7\overline{q}_7\overline{q}_7^*)\},\\
g_{02} = \frac{2}{\bar{\rho}}\{&m_{18}(\overline{q}_1^2\overline{q}_1^* + \overline{q}_5^2\overline{q}_5^*) + m_{21}(\overline{q}_2^2\overline{q}_2^* + \overline{q}_6^2\overline{q}_6^*) + m_{31}(\overline{q}_3^2\overline{q}_3^* + \overline{q}_7^2\overline{q}_7^*)\\
&+ m_{43}(\overline{q}_4^2\overline{q}_4^* + \overline{q}_8^2\overline{q}_8^*) + e^{2i\omega_c\tau_1}[(m_{11}\overline{q}_3^2 + m_{12}\overline{q}_3\overline{q}_8 + m_{13}\overline{q}_8^2)\overline{q}_1^*\\
&+ (m_{13}\overline{q}_4^2 + m_{12}\overline{q}_4\overline{q}_7 + m_{11}\overline{q}_7^2)\overline{q}_5^*] + e^{2i\omega_c\tau_4}m_{41}(\overline{q}_3^2\overline{q}_4^* + \overline{q}_7^2\overline{q}_8^*)\},
\end{aligned}$$

$$\begin{aligned}
g_{21} = \frac{1}{\bar{\rho}}\{&6m_{19}(q_1^2\overline{q}_1\overline{q}_1^* + q_5^2\overline{q}_5\overline{q}_5^*) + 6m_{22}(q_2^2\overline{q}_2\overline{q}_2^* + q_6^2\overline{q}_6\overline{q}_6^*)\\
&+ 6m_{32}(q_3^2\overline{q}_3\overline{q}_3^* + q_7^2\overline{q}_7\overline{q}_7^*) + 6m_{44}(q_4^2\overline{q}_4\overline{q}_4^* + q_8^2\overline{q}_8\overline{q}_8^*)\\
&+ 4m_{18}(q_1\overline{q}_1^*w_{11}^{(1)}(0) + q_5\overline{q}_5^*w_{11}^{(5)}(0))\\
&+ 4m_{21}(q_2\overline{q}_2^*w_{11}^{(2)}(0) + q_6\overline{q}_6^*w_{11}^{(6)}(0))\\
&+ 4m_{31}(q_3\overline{q}_3^*w_{11}^{(3)}(0) + q_7\overline{q}_7^*w_{11}^{(7)}(0))\\
&+ 4m_{43}(q_4\overline{q}_4^*w_{11}^{(4)}(0) + q_8\overline{q}_8^*w_{11}^{(8)}(0))\\
&+ e^{-i\omega_c\tau_4}[6m_{42}q_3^2\overline{q}_3\overline{q}_4^* + 4m_{41}q_3\overline{q}_4^*w_{11}^{(3)}(-\tau_4)\\
&+ 2q_7\overline{q}_8^*(3m_{42}q_7\overline{q}_7 + 2m_{41}w_{11}^{(7)}(-\tau_4))]\\
&+ 2e^{-i\omega_c\tau_1}[(3m_{14}q_3^2 + q_8(2m_{15}q_3 + m_{16}q_8))\overline{q}_3\overline{q}_1^*\\
&+ (m_{15}q_3^2 + q_8(2m_{16}q_3 + 3m_{17}q_8))\overline{q}_8\overline{q}_1^*
\end{aligned}$$

$$
\begin{aligned}
&+(2m_{11}q_3+m_{12}q_8)\overline{q}_1^*w_{11}^{(3)}(-\tau_1)\\
&+\overline{q}_5^*((3m_{17}q_4^2+q_7(2m_{16}q_4+m_{15}q_7))\overline{q}_4\\
&+(m_{16}q_4^2+2m_{15}q_4q_7+3m_{14}q_7^2)\overline{q}_7+(2m_{13}q_4+m_{12}q_7)w_{11}^{(4)}(-\tau_1)\\
&+(m_{12}q_4+2m_{11}q_7)w_{11}^{(7)}(-\tau_1))+(m_{12}q_3+2m_{13}q_8)\overline{q}_1^*w_{11}^{(8)}(-\tau_1)]\\
&+2m_{18}(\overline{q}_1\overline{q}_1^*w_{20}^{(1)}(0)+\overline{q}_5\overline{q}_5^*w_{20}^{(5)}(0))\\
&+2m_{21}(\overline{q}_2\overline{q}_2^*w_{20}^{(2)}(0)+\overline{q}_6\overline{q}_6^*w_{20}^{(6)}(0))\\
&+2m_{31}(\overline{q}_3\overline{q}_3^*w_{20}^{(3)}(0)+\overline{q}_7\overline{q}_7^*w_{20}^{(7)}(0))\\
&+2m_{43}(\overline{q}_4\overline{q}_4^*w_{20}^{(4)}(0)+\overline{q}_8\overline{q}_8^*w_{20}^{(8)}(0))\\
&+2e^{i\omega_c\tau_4}m_{41}(\overline{q}_3\overline{q}_4^*w_{20}^{(3)}(-\tau_4)+\overline{q}_7\overline{q}_8^*w_{20}^{(7)}(-\tau_4))\\
&+e^{i\omega_c\tau_1}[\overline{q}_5^*((2m_{13}\overline{q}_4+m_{12}\overline{q}_7)w_{20}^{(4)}(-\tau_1)\\
&+m_{12}\overline{q}_4+2m_{11}\overline{q}_7)w_{20}^{(7)}(-\tau_1))\\
&+\overline{q}_3\overline{q}_1^*(2m_{11}w_{20}^{(3)}(-\tau_1)+m_{12}w_{20}^{(8)}(-\tau_1))\\
&+\overline{q}_8\overline{q}_1^*(m_{12}w_{20}^{(3)}(-\tau_1)+2m_{13}w_{20}^{(8)}(-\tau_1))]\},
\end{aligned}
$$

where $w_{20}^{(k)}(\theta)$ and $w_{11}^{(k)}(\theta)$ are the kth components of $w_{20}(\theta)$ and $w_{11}(\theta)$ respectively. And for $-\tau_M\le\theta<0$, it can be computed that

$$
\begin{cases}
w_{20}(\theta)=\frac{ig_{20}}{\omega_c}q(0)e^{i\omega_c\theta}-\frac{\bar{g}_{02}}{3i\omega_c}\bar{q}(0)e^{-i\omega_c\theta}+E_1e^{2i\omega_c\theta}\\
w_{11}(\theta)=\frac{g_{11}}{i\omega_c}q(0)e^{i\omega_c\theta}-\frac{\bar{g}_{11}}{i\omega_c}\bar{q}(0)e^{-i\omega_c\theta}+E_2,
\end{cases}
$$

where

$$
\begin{aligned}
E_1=&\left(2i\omega_cI-\int_{-\tau_M}^{0}e^{2i\omega_c\theta}d\eta(\theta,0)\right)^{-1}\\
&\begin{pmatrix}
2[m_{18}q_1^2+e^{-2i\omega_c\tau_1}(m_{11}q_3^2+q_8(m_{12}q_3+m_{13}q_8))]\\
2m_{21}q_2^2\\
2m_{31}q_3^2\\
2(e^{-2i\omega_c\tau_4}m_{41}q_3^2+m_{43}q_4^2)\\
2[m_{18}q_5^2+e^{-2i\omega_c\tau_1}(m_{13}q_4^2+q_7(m_{12}q_4+m_{11}q_7))]\\
2m_{21}q_6^2\\
2m_{31}q_7^2\\
2(e^{-2i\omega_c\tau_4}m_{41}q_7^2+m_{43}q_8^2)
\end{pmatrix},\\
E_2=&\left[-\int_{-\tau_M}^{0}d\eta(\theta,0)\right]^{-1}
\end{aligned}
$$

$$\begin{pmatrix} 2m_{18}q_1\overline{q}_1 + 2m_{11}q_3\overline{q}_3 + m_{12}(q_8\overline{q}_3 + q_3\overline{q}_8) + 2m_{13}q_8\overline{q}_8 \\ 2m_{21}q_2\overline{q}_2 \\ 2m_{31}q_3\overline{q}_3 \\ 2m_{41}q_3\overline{q}_3 + 2m_{43}q_4\overline{q}_4 \\ 2m_{13}q_4\overline{q}_4 + m_{12}(q_7\overline{q}_4 + q_4\overline{q}_7) + 2m_{18}q_5\overline{q}_5 + 2m_{11}q_7\overline{q}_7 \\ 2m_{21}q_6\overline{q}_6 \\ 2m_{31}q_7\overline{q}_7 \\ 2m_{41}q_7\overline{q}_7 + 2m_{43}q_8\overline{q}_8 \end{pmatrix}.$$

With g_{20}, g_{11}, g_{02}, and g_{21}, we can compute $C_1(r_c)$, p_2, ζ_2, and T_2 for the stability and the other properties for the bifurcating periodic solution.

References

Asada T, Yoshida H (2003) Coefficient criterion for four-dimensional Hopf bifurcations: a complete mathematical characterization and applications to economic dynamics. Chaos Solitons Fractals 18:525–536

Ay A, Knierer S, Sperlea A, Holland J, Özbudak EM (2013) Short-lived Her proteins drive robust synchronized oscillations in the zebrafish segmentation clock. Development 140(15):3244–3253

Ay A, Holland J, Sperlea A, Devakanmalai GS, Knierer S, Sangervasi S, Stevenson A, Özbudak EM (2014) Spatial gradients of protein-level time delays set the pace of the traveling segmentation clock waves. Development 141(21):4158–4167

Baker RE, Schnell S, Maini PK (2006) A mathematical investigation of a clock and wavefornt model for somitogenesis. J Math Biol 52(4):458–482

Baker RE, Schnell S (2009) How can mathematics help us explore vertebrate segmentation? HFSP 3(1):1–5

Campanelli M, Gedeon T (2010) Somitogenesis clock-wave initiation requires differential decay and multiple binding sites for clock protein. PLoS Comput Biol 6(4):e1000728

Cinquin O (2007) Repressor dimerization in the zebrafish somitogenesis clock. PLoS Comput Biol 3(2):e32

Cooke J, Zeeman EC (1976) A clock and wavefront model for control of the number of repeated structures during animal morphogenesis. J Theor Biol 58(2):455–476

Dubrulle J, McGrew MJ, Pourquié O (2001) FGF signalling controls somite boundary position and regulates segmentation clock control of spatiotemporal Hox gene activation. Cell 106(2):219–232

Dubrulle J, Pourquié O (2002) From head to tail: links between the segmentation clock and antero-posterior patterning of the embryo. Curr Opin Genet Dev 12(5):519–523

Ermentrout GB, Terman DH (2010) Mathematical foundations of neuroscience. Springer, New York

Goldbeter A, Pourquié O (2008) Modeling the segmentation clock as a network of coupled oscillations in the Notch, Wnt and FGF signaling pathways. J Theor Biol 252(3):574–585

Görlich D, Kutay U (1999) Transport between the cell nucleus and the cytoplasm. Annu Rev Cell Dev Biol 15:607–660

Hanneman E, Westerfield M (1989) Early expression of acetyl-choline-sterase activity in functionally distinct neurons of the zebrafish. J Comp Neurol 284(3):350–361

Hassard BD, Kazarinoff ND, Wan YH (1981) Theory and applications of Hopf bifurcation. Cambridge University, Cambridge, New York

Herrgen L, Ares S, Morelli LG, Schröter C, Jülicher F, Oates AC (2010) Intercellular coupling regulates the period of the segmentation clock. Curr Biol 20(14):1244–1253

Holley SA (2007) The genetics and embryology of zebrafish metamerism. Dev Dyn 236(6):1422–1449

Horikawa K, Ishimatsu K, Yoshimoto E, Kondo S, Takeda H (2006) Noise-resistant and synchronized oscillation of the segmentation clock. Nature 441(7094):719–723

Jenkins RP, Hanisch A, Soza-Ried C, Sahai E, Lewis J (2015) Stochastic regulation of her1/7 gene expression is the source of noise in the zebrafish somite clock counteracted by Notch signalling. PLoS Comput Biol 11(11):e1004459

Jiang YJ, Aerne BL, Smithers L, Haddon C, Ish-Horowicz D, Lewis J (2000) Notch signaling and the synchronization of the somite segmentation clock. Nature 408(6811):475–479

Kawamura A, Koshida S, Hijikata H, Sakaguchi T, Kondoh H, Takada S (2005) Zebrafish hairy/enhancer of split protein links FGF signaling to cyclic gene expression in the periodic segmentation of somites. Genes Dev 19(10):1156–1161

Kuramoto Y (1984) Chemical oscillations, waves, and turbulence. Springer, Berlin

Lewis J (2003) Autoinhibition with transcriptional delay: a simple mechanism for the zebrafish somitogenesis oscillator. Curr Biol 13(16):1398–1408

Liao KL (2012) Analysis on mathematical models of somitogenesis in zebrafish. Dissertation, National Chiao Tung University, Taiwan

Liao KL, Shih CW (2012) A lattice model on somitogenesis of zebrafish. Discrete Contin Dyn Syst B 17(8):2789–2814

Liao KL, Shih CW, Tseng JP (2012) Synchronized oscillations in mathematical model of segmentation in zebrafish. Nonlinearity 25:869–904

Makarov DE (2009) Computer simulations and theory of protein translocation. Acc Chem Res 42(2):281–289

Mara A, Schroeder J, Chalouni C, Holley SA (2007) Priming, initiation and synchronization of the segmentation clock by deltaD and deltaC. Nat Cell Biol 9(5):523–530

Morelli LG, Ares S, Herrgen L, Schröter C, Jölicher F, Oates AC (2009) Delayed coupling theory of vertebrate segmentation. HFSP 3(1):55–66

Murray JD (2002) Mathematical biology. Springer, New York

Özbudak EM, Lewis J (2008) Notch signalling synchronizes the zebrafish segmentation clock but is not needed to create somite boundaries. PLoS Genet 4(2):e15

Pourquié O (2004) The chick embryo: a leading model in somitogenesis studies. Mech Dev 121(9):1069–1079

Riedel-Kruse IH, Müller C, Oates AC (2007) Synchrony dynamics during initiation, failure, and rescue of the segmentation clock. Science 317(5846):1911–1915

Schröter C, Ares S, Morelli LG, Isakova A, Hens K, Soroldoni D, Gajewski M, Jülicher F, Maerkl SJ, Deplancke B, Oates AC (2012) Topology and dynamics of the zebrafish segmentation clock core circuit. PLoS Biol 10(7):e1001364

Schwendinger-Schreck J, Kang Y, Holley SA (2014) Modeling the zebrafish segmentation clock's gene regulatory network constrained by expression data suggests evolutionary transitions between oscillating and nonoscillating transcription. Genetics 197(2):725–738

Simon SM, Peskin CS, Oster GF (1992) What drives the translocation of proteins? PNAS 89(9):3770–3774

Shih CW, Tseng JP (2008) Convergent dynamics for multistable delayed neural networks. Nonlinearity 21:2361–2389

Shih CW, Tseng JP (2011) Global synchronization and asymptotic phases for a ring of identical cells with delayed coupling. SIAM J Math Anal 43(4):1667–1697

Sieger D, Ackermann B, Winkler C, Tautz D, Gajewski M (2006) her1 and her13.2 are jointly required for somitic border specification along the entire axis of the fish embryo. Dev Biol 293:242–251

Uriu K, Morishita Y, Iwasa Y (2009) Traveling wave formation in vertebrate segmentation. J Theor Biol 257(3):385–396

Uriu K, Morishita Y, Iwasa Y (2010) Synchronized oscillation of the segmentation clock gene in vertebrate development. J Math Biol 61:207–229

Yeung HKS, Strogatz SH (1999) Time delay in the Kuramoto model of coupled oscillators. Phys Rev Lett 82:648–651

Yu W, Cao J (2006) Stability and Hopf bifurcation analysis on a four-neuron BAM neural network with time delays. Phys Lett A 351:64–78

Zeiser S, Müller J, Liebscher V (2007) Modeling the Hes1 oscillator. J Comput Biolo 14(7):984–1000